A Second Role for the Second Messenger Cyclic-di-GMP in *E. coli*: Arresting Cell Growth by Altering Metabolic Flow

YuneSahng Hwang and Rasika M. Harshey*

Department of Molecular Biosciences

University of Texas at Austin

Austin, TX 78712

*Correspondence to: rasika@austin.utexas.edu

Running title: A second role for the second messenger c-di-GMP

Abstract

C-di-GMP primarily controls motile to sessile transitions in bacteria. Diguanylate cyclases (DGCs) catalyze the synthesis of c-di-GMP from two GTP molecules. Typically, bacteria encode multiple DGCs that are activated by specific environmental signals. Their catalytic activity is modulated by c-di-GMP binding to autoinhibitory sites (I-sites). YfiN is a conserved inner membrane DGC that lacks these sites. Instead, YfiN activity is directly repressed by periplasmic YfiR, which is inactivated by redox stress. In *E. coli*, an additional envelope stress causes YfiN to relocate to the mid-cell to inhibit cell division by interacting with the division machinery. Here, we report a third activity for YfiN in *E. coli*, where cell growth is inhibited without YfiN relocating to the division site. This action of YfiN is only observed when the bacteria are cultured on gluconeogenic carbon sources, and is dependent on absence of the autoinhibitory sites. Restoration of I-site function relieves the growth-arrest phenotype, and disabling this function in a heterologous DGC causes acquisition of this phenotype. Arrested cells are tolerant to a wide range of antibiotics. We show that the likely cause of growth arrest is depletion of cellular GTP from run-away synthesis of c-di-GMP, explaining the dependence of growth arrest on gluconeogenic carbon sources that exhaust more GTP during production of glucose. This is the first report of c-di-GMP-mediated growth arrest by altering metabolic flow.

38 **Significance**

39 The c-di-GMP signaling network in bacteria not only controls a variety of cellular processes
40 such as motility, biofilms, cell development and virulence, but does so by a dizzying array of
41 mechanisms. The DGC YfiN singularly represents the versatility of this network in that it not
42 only inhibits motility and promotes biofilms, but also arrests growth in *E. coli* by relocating to
43 the mid-cell and blocking cell division. The work described here reveals that YfiN arrests
44 growth by yet another mechanism in *E. coli* – changing metabolic flow. This function of YfiN,
45 or of DGCs without autoinhibitory I-sites, may contribute to antibiotic tolerant persisters in
46 relevant niches such as the gut where gluconeogenic sugars are found.

Introduction

Bacteria show a remarkable ability to adapt to different environmental conditions through multiple signaling networks [1, 2]. Some of these networks commonly use cyclic or linear nucleotides to link environmental stimuli to specific bacterial responses [3, 4]. Cyclic di-GMP (c-di-GMP) was first identified in *Gluconacetobacter xylinus* for its role in cellulose production [5]. In most bacteria c-di-GMP controls the transition between motile and sessile behaviors, but is not limited to these functions [6, 7]. Broader roles for this system include virulence, progression through the cell cycle, phage resistance, and surface attachment [8-11].

Intracellular c-di-GMP levels are regulated by multiple diguanylate cyclases (DGCs) identifiable by a signature GGDEF active-site (referred to as GGDEF domain) that catalyze the synthesis of c-di-GMP from two GTP molecules, and multiple phosphodiesterases (PDEs) identifiable by EAL or HD-GYP domains that break down c-di-GMP first to linear pGpG and subsequently to GMP [12, 13]. Although ectopic expression of most DGCs and PDEs often leads to dramatic phenotypes, their native expression often does not, as observed by lack of an observable phenotype when their genes are experimentally mutated, indicating that these enzymes may be only activated under specific environmental conditions. The presence of specific sensory modules such as HAMP, PAS, LuxR or BLUF domains allows these enzymes to respond to a variety of sensory cues, both chemical and physical; however, most signals activating these enzymes are still unknown [14-18]. The c-di-GMP produced in response to these signals elicits its varied outputs primarily by binding to cellular effectors and targets.

DGCs are regulated not only by environmental signals but can also self-regulate. An autoinhibition (I) site located close to the active site was first identified in the DGC PleD of *Caulobacter crescentus*, where it regulates enzyme activity through negative feed-back, curtailing excess c-di-GMP production [12]. This site (primary I site; I_p) is identifiable by an RXXD consensus located five amino acids upstream of the GGDEF motif. c-di-GMP bound at I_p causes a conformation change that leads to the repression of enzymatic activity; accordingly,

73 mutations in conserved I_p residues increase c-di-GMP production [12]. Based on structural
74 studies, additional arginine residues located outside the GGDEF domain in PleD were also
75 seen to contribute to the c-di-GMP pocket for feedback inhibition; these were designated the
76 secondary I site (I_s) [19]. A different role for I_s was reported for the DGC GcbC in *Pseudomonas*
77 *fluorescens*, where this site is required for interaction of GcbC with its target protein LapD,
78 which controls biofilm production [20].

79 YfiN, also called DgcN or TpbB, is a conserved inner membrane DGC with a Per-Arnt-
80 Sim (PAS)-like sensory domain in the periplasm and HAMP-GGDEF domains in the cytoplasm
81 [21, 22]. *E. coli* YfiN lacks both I_p and I_s sites, as do the majority of bacterial YfiN homologs. In
82 *E. coli, Salmonella enterica* and *Pseudomonas aeruginosa*, the enzymatic activity of YfiN is
83 repressed by periplasmic YfiR [16, 23, 24]. Redox stress can cause YfiR to dissociate from
84 YfiN, activating its DGC function [16, 24]. In *P. aeruginosa*, transposon disruption of *yfiR* led
85 to increased biofilm formation through the Pel/Psl biosynthesis pathway, and enzymatically
86 inactive YfiN showed less virulence in the mouse model compared to wild-type (WT) [16]. YfiN
87 was also shown to be important for biofilm maintenance in response to peroxide stress in *P.*
88 *aeruginosa* [25].

89 In *E. coli*, YfiN exhibits the canonical motility-inhibition function of a DGC [24]. A
90 second very different function for YfiN is a two-step response to redox and envelope stresses:
91 in response to redox stress YfiN produces c-di-GMP, and in response to a second envelope
92 stress YfiN moves to the mid-cell to arrest cell division [24]. Unlike known cell division inhibitors
93 [26], the interaction of YfiN with cell division proteins FtsZ and ZipA retains the Z ring at the
94 mid-cell but prevents septal invagination [24]. We report here a third function for YfiN in *E. coli,*
95 where YfiN arrests growth by a mechanism different from cell division arrest. This mechanism
96 exploits the absence of regulatory I sites in this DGC. We show that when growing on
97 gluconeogenic sugars, unregulated c-di-GMP synthesis by YfiN depletes cellular GTP, which
98 is the likely cause of failure of all macromolecular synthesis. Growth arrest can be reversed

99 by reintroducing the I sites. Such a function for a DGC has not been previously reported in
100 bacteria. This ability of YfiN to enable survival by shutting down growth, allows the bacteria to
101 tolerate a broad spectrum of antibiotics.

102

103 Results

104 YfiN arrests *E. coli* growth on specific carbon sources

105 Prior studies conducted in *E. coli* growing in LB with ectopically expressed YfiN reported that
106 even though expression was induced from the beginning of a growth cycle, YfiN appeared at
107 the division site just prior to the onset of the stationary phase, resulting in cell division arrest
108 [24]. When cells were grown in minimal M9 glycerol (M9M) however, we observed that
109 irrespective of whether the ectopic expression was from a plasmid (pYfiN; PBAD promoter) or
110 from its chromosomal location (cYfiN$_{GFP}$; PTrc promoter; all cYfiN experiments were with the
111 GFP-tagged version and will be referred to as cYfiN henceforth), growth began to slow as
112 early as two hours post-YfiN induction and to remain arrested (**Fig. 1A, B**); western blot
113 analysis showed cYfiN levels to be ~8 fold lower than pYfiN (**Fig. S1A**). The DGC function of
114 YfiN was important for this phenotype, as observed by lack of growth arrest in the active site
115 mutant pYfiN(GGAAF), where the GGDEF signature motif is changed to GGAAF **(Fig. 1C**);
116 this mutation did not compromise protein stability (**Fig. S1B**).

117 To test whether localization of YfiN to the mid-cell is required for the growth arrest
118 observed in Figure 1 (**A,B**), the location of both cYfiN and pYfiN$_{GFP}$ was monitored in M9M.
119 cYfiN was found dispersed throughout the cell, while pYfiN$_{GFP}$ relocated to the mid-cell in 60%
120 of the cells (**Fig. 2A**). Thus, the observed growth-arrest by cYfiN is not related to its ability to
121 localize at the division site, while that of pYfiN$_{GFP}$ may include division arrest (**Fig. 1A, B**). To
122 investigate if the mid-cell localization of pYfiN$_{GFP}$ in 60% of the cells was related to the higher

123 expression levels from a plasmid, we monitored the behavior of a plasmid encoded R260A
124 mutant of YfiN (R260 is located in the cytoplasmic domain) that does not localize to the mid-
125 cell (**Fig. 2B;** see **Fig. S1B** for protein expression). Like pYfiN$_{GFP}$, pYfiN(R260A)$_{GFP}$ induction
126 resulted in severe motility inhibition on soft agar plates, indicating robust c-di-GMP production
127 (**Fig. 2C**). Despite its failure to localize to the mid-cell, the R260A mutant arrested growth
128 similar to WT YfiN (**Fig. 2D**). We conclude that the inability to grow in M9M is a new phenotype
129 of YfiN, distinct from its ability to arrest cell division by interacting with the divisome at the mid-
130 cell.

131 *E. coli* has 12 DGCs, of which five (including YfiN) harbor a transmembrane region.
132 To test if this new phenotype of YfiN is related to its membrane location, and to also control
133 for overexpression artifacts, we cloned the other four transmembrane DGCs (C, E, F and J)
134 [27] under PBAD control. In contrast to YfiN, none of these four DGCs arrested growth in M9M
135 (**Fig. 2E**). Except for DgcF, the ectopic expression of DgcC, E and J inhibited motility,
136 suggesting that they were active as DGCs (**Fig. 2F)**, which is supported by previous work [28-
137 30]. We conclude that early growth arrest in M9M is unique to YfiN.

138 A clear difference between the early growth-arrest observed in this study (**Fig. 1A,B**)
139 and the late growth-arrest phenotype of YfiN reported earlier [24] was the growth medium:
140 minimal M9M in the present study, and nutrient-rich LB in the earlier one. When glycerol was
141 substituted with glucose, the most favored carbon source for *E. coli*, cYfiN no longer inhibited
142 growth in M9M (**Fig. 1D**, third set of bars from the left). In *E. coli* growing aerobically, glucose
143 is directly integrated into glycolysis as glucose 6-phosphate (G6P) and consumed through the
144 tricarboxylic acid cycle (TCA), while glycerol, an energy-poor carbon source is incorporated
145 into central metabolism as dihydroxyacetone phosphate (DHAP), a metabolite that can
146 participate in both gluconeogenic and glycolytic processes [31] (**Fig. 1E**). To explore this
147 finding further, we provided several gluconeogenic and non-gluconeogenic substrates as
148 carbon sources in the M9 medium. For the former we chose G6P, lactose, glucose and

149 arabinose, and for the latter we chose the following: sugar alcohols in addition to glycerol
150 (sorbitol, mannitol), various other sugars (fructose, mannose, maltose), acetate, and TCA
151 cycle intermediates (pyruvate, succinate). There was a clear-cut difference in the ability of YfiN
152 to arrest growth on the two sets of carbon sources, which was patterned after the glycerol and
153 glucose examples i.e. only gluconeogenic sugars arrested growth. If the differential growth
154 arrest phenotype of YfiN on these two types of substrates is because of the higher energy
155 produced by one substrate type versus the other, the expectation is that providing both
156 substrates would override the effect of the gluconeogenic substrate. This was found to be the
157 case (**Fig. S2A-D**). To test whether YfiN-mediated growth arrest is reversible, either glucose
158 or LB was added 2 hours post-induction of YfiN. Bacteria resumed growth immediately,
159 suggesting that YfiN-mediated growth arrest is fully reversible and that cells are not dead (**Fig.**
160 **S2E**).

161

162 **Growth arrest is correlated with absence of autoinhibitory I sites in YfiN**

163 Given that the DGC activity of YfiN is required to mediate growth arrest (**Fig. 1C**), we first
164 tested whether the canonical function of c-di-GMP (turning on biofilm pathways / shutting down
165 motility) played a role. This was done in two ways: 1) simultaneous expression of YfiN with
166 YhjH (the most active PDE in *E. coli*) expected to degrade c-di-GMP and 2) disruption of six
167 key genes that control the major biofilm pathways in *E. coli* (production of cellulose, PGA,
168 colanic acid, Type 1 fimbriae, EPS etc.) [32]. In the first case, i.e. expression of YhjH, the
169 inhibitory effect of YfiN on motility was substantially relieved (**Fig. S3A**); the reduction in c-di-
170 GMP levels was confirmed using a riboswitch-based biosensor (see Methods) [33, 34] (**Fig.**
171 **S3B**). Yet, the growth arrest function of YfiN was not relieved (**Fig. S3C**). In the second case,
172 i.e. disruption of multiple biofilm pathways, biofilm levels decreased as expected (**Fig. S3D**).
173 However, YfiN still arrested growth (**Fig. S3E**). In summary, the canonical functions of c-di-

174 GMP do not contribute to the observed growth arrest phenotype of YfiN.

175 In thinking about what distinguishes YfiN from the all the other inner membrane *E. coli*
176 DGCs previously tested (Dgc C, E, F, J), we noted that YfiN lacks the consensus autoinhibitory
177 I site residues (I_p and I_s), which bind c-di-GMP to feedback regulate enzyme activity (**Fig. 3AB**)
178 [12, 35]. We reasoned that lack of autoregulation would lead to continual c-di-GMP production,
179 hence depletion of cellular GTP. Depletion of GTP as a mechanism of growth arrest is well-
180 established in the (p)pGpp-mediated pathway [36]. Imbalance in nucleotide pools is also
181 known to disrupt growth [37, 38]. To test the GTP depletion idea, we rebuilt the two YfiN I sites
182 (I_p and I_s) both sequentially and together. I_p was restored by changing GLRH to the consensus
183 RXXD, and I_s by changing N280 to R. Only when both I sites were reconstituted, was growth
184 arrest fully reversed (**Fig. 3C**). These changes did not perturb either the DGC activity of the I-
185 site reconstituted strains as monitored by motility inhibition in soft agar plates (**Fig. 3D**) or by
186 protein expression levels (I_{ps} mutant; **S1B**). We also measured c-di-GMP levels in YfiN and its
187 mutants using the riboswitch-based biosensor. As expected, introduction of I site mutations
188 reduced enzymatic function (I_p and I_s), with I_{ps} showing the lowest c-di-GMP levels (**Fig. S4**).
189 To test whether the I-site is integral to the growth arrest phenotype, we mutated the I_p site
190 (RESD → GESD) in DgcA, a robust heterologous DGC from *C. crescentus* [12]. Expression
191 of WT DgcA in *E. coli* did not elicit growth arrest in M9M, but expression of the DgcA I_p mutant
192 did (**Fig. 3E**). We note that c-di-GMP levels in DgcA were similar to those when YhjH was co-
193 expressed with YfiN (**Fig. S3B**), yet growth arrest was seen in the latter i.e. YfiN + YhJH (**Fig.
194 S3C**) but not the former i.e. DgcA (**Fig. 3E**). Thus, both loss of the growth-arrest phenotype in
195 YfiN and gain of this phenotype by DgcA by merely restoring and inactivating I-site function,
196 respectively, allows us to conclude that unregulated c-di-GMP production in the absence of
197 the I site is responsible for the arrest not by increasing c-di-GMP levels per se, but likely by
198 depleting cellular GTP levels through continuous c-di-GMP synthesis.

199

200 **YfiN expression depletes intracellular GTP**

201 To test our conjecture that GTP depletion due to unregulated c-di-GMP synthesis is the cause
202 of growth arrest by YfiN, we first compared cellular nucleotide levels with (+) or without (-)
203 induction of $_{c}$YfiN by metabolomic analysis of a standard panel of 219 intracellular metabolites.
204 Of these, the levels of five ribonucleotides relevant to this study are shown in **Figure 4AB**. c-
205 di-GMP levels were high in the cYfiN+ strain as expected. A consistent decrease in the levels
206 of GTP, ATP, UTP and CTP was seen in experimental samples compared to the controls. To
207 confirm the drop in GTP concentration upon cYfiN expression, we next used a luciferase-
208 linked GTP assay (GTPase-Glo™), which converts GTP into ATP, the latter detected by the
209 light produced by the luciferase reaction (**Fig. 4C**)**.** We observed a 50% decrease in GTP
210 levels in cYfiN-expressing cells, supporting the GTP metabolomics data. To monitor GTP
211 levels by a third method, as well as to test the proficiency of various YfiN I-site mutants in
212 converting GTP to c-di-GMP, cell lysates expressing pYfiN and its I-site double mutant (I_{ps})
213 variant were incubated with [α-^{32}P] GTP at regular time intervals from 0-15 min and the
214 products analyzed by thin layer chromatography (TLC); only data for the 10 min time point are
215 shown because in this experiment, WT pYfiN lysates depleted almost all of the input GTP at
216 this time, while ~20% of input GTP still remained in the I_{ps} mutant (**Fig. 4D**). We then compared
217 the time course of GTP consumption by WT pYfiN with that of I-site regulated pDgcA (**Fig. 4E**).
218 By16 min, YfiN had consumed most of the GTP, while half of the input GTP still remained
219 during DgcA expression. This difference in enzymatic activity may be critical when intracellular
220 GTP is low to begin with in glycerol-fed cells (~2.5 fold lower compared to glucose) [39]. We
221 finally used a fourth method to verify GTP depletion by quantifying the absolute levels of GTP
222 using mass spec as described under Methods. GTP levels decreased significantly in cells
223 expressing pYfiN (**Fig. 4F**). Although $_{p}$YfiN(I_{ps}) and $_{p}$DgcA cells showed higher levels of GTP
224 compared to $_{p}$EmptyVector, the difference was not statistically significant. Thus, four different
225 kinds of measurements show that YfiN expression depletes cellular GTP as expected. The

226 data in Fig. 4B show that YfiN expression impacts all ribonucleotide triphosphate levels as
227 well.

228 An alternative explanation for the depletion of cellular GTP observed in Figure 4 could
229 be activation of the (p)ppGpp synthesis pathway, during which a diphosphate from ATP is
230 transferred to the 3′-OH oxygen of GTP/GDP; (p)ppGpp is the primary regulator of GTP
231 homeostasis in *E. coli* [39], and deployed in bacteria experiencing various stresses [40, 41].
232 In *E. coli*, RelA and SpoT are the only known enzymes that synthesize as well as degrade
233 (p)ppGpp, which is not made in the absence of both proteins ($ppGpp^0$) [42]. To test this
234 alternate explanation, we induced YfiN in *ΔrelA* or *ΔrelAΔspoT*($ppGpp^0$) background,
235 expected to have minimal amounts of (p)ppGpp. Both mutant strains showed growth arrest as
236 early as 2 hours after induction of YfiN (**Fig. S5**), ruling out involvement of (p)ppGpp in YfiN-
237 induced arrest.

238 To run an independent check of studies concluding that less GTP is available during
239 growth on poor carbon sources such as glycerol and acetate [43], we considered tweaking
240 enzymes contributing to gluconeogenesis. We chose phosphoenolpyruvate carboxy kinase
241 (PCK) for our test, as it mediates an irreversible step in the pathway, converting oxaloacetate
242 to phosphoenolpyruvate, and promotes gluconeogenesis [44] (**Fig. S6A**). Increasing PCK
243 levels might therefore be expected to increase severity of the growth arrest. We monitored
244 growth in M9 mannitol, where cYfiN-mediated growth arrest is not as severe as in M9M (**Fig.
245 1E**). In this growth medium, PCK induction resulted in a severity of growth arrest similar to that
246 seen in M9M (**Fig. S6B)**. These data, along with those demonstrating that YfiN-mediated
247 growth arrest can be reversed by the addition of a non-gluconeogenic sugar (**Fig. S2E**),
248 support our hypothesis that the availability of GTP pools underlies the mechanism of the YfiN-
249 mediated growth arrest.

250 In summary, we infer from the data in this and prior sections that absence of feed-

251 back control of c-di-GMP synthesis in YfiN, combined with the energy-expensive metabolism
252 of gluconeogenic sugars, deplete cellular GTP to levels unsustainable for growth, which can
253 be rescued by utilizing non-gluconeogenic sugars.

254

255 **YfiN-arrested cells are tolerant to a broad class of antibiotics**

256 To investigate whether all major cellular processes - cell wall, protein and DNA synthesis – are
257 arrested by YfiN during growth on M9M, we exposed cells to the antibiotics Ampicillin,
258 Gentamicin, and Ciprofloxacin [45]. At the bactericidal concentrations used, $_{c}$YfiN-expressing
259 cells survived better than control cells in the presence of all three antibiotics when tested as
260 follows. Cells were first grown with or without cYfiN induction on M9M + antibiotic plates for
261 12 hours (**Fig. 5A,** middle). They were then transferred with an inoculation loop to LB plates
262 without added antibiotics for recovery (**Fig. 5A,** right; Gen/Amp/Cip stamps only point to the
263 antibiotic condition from where cells were taken). The results are shown in **Figure 5B** (note
264 again that there are no antibiotics in these plates, as illustrated in Fig. 5A, right). Without cYfiN
265 expression, cells succumbed to all three antibiotics they were initially plated on, as judged by
266 loss of recovery of viable cells (**Fig. 5B, left**); this was not the case when cYfiN was expressed
267 (**Fig. 5B, right**). To quantify the number of YfiN-expressing cells that survive antibiotic
268 treatment, a similar assay was performed in M9M, where after 4 hours of antibiotic exposure,
269 survival was measured by CFU counts on LB plates (**Fig. 5C, D**). The results were similar to
270 those reported in Fig. 5B i.e YfiN-expression increases survival to multiple antibiotics. We
271 conclude that YfiN effectively shuts down all major cellular processes in M9M.

272 Since the enzymatic function of YfiN is closely related to the growth arrest phenotype,
273 we reasoned that this function should also be linked to its antibiotic tolerance property. This
274 was tested in two ways using $_{c}$YfiN – by concomitantly increasing the expression of its
275 periplasmic inhibitor YfiR (pYfiR) (**Fig. S7A**), as well as by testing the GGDEF active site

276 mutant (**Fig. S7B**). Both manipulations abrogated the antibiotic (Cip) tolerance phenotype. We
277 conclude that the DGC activity of YfiN mediates both growth arrest and antibiotic tolerance.

278

279 **Native YfiN delays exit from lag phase during exponential growth**

280 The results presented thus far have relied on ectopic expression of YfiN from non-native
281 promoters, either from the chromosome or from a plasmid. But are they relevant to the native
282 situation? Since we do not know what environmental conditions induce native YfiN, we took
283 advantage of a report that showed a brief burst of YfiN protein levels when overnight cultures
284 are inoculated into fresh media [46]. We therefore prepared overnight cultures of WT and
285 *ΔyfiN* strains in LB, and inoculated them to either M9 glycerol or M9 glucose, recording their
286 growth rates over three 2-hour intervals are shown in **Fig. 6AB (***ΔyfiN* data are in orange). In
287 M9 glycerol (**Fig. 6A**), both strains were still in the lag phase in the first growth interval (0-2
288 hour). In the next interval (2-4 hour), the growth rate of WT was unchanged i.e. it was still in
289 the lag phase, but that of the *ΔyfiN* strain increased. In the third interval or exponential phase
290 of growth (4-6 hour), both strains grew at the same rate. Thus, the WT strain showed a longer
291 lag or delayed transition to exponential phase compared to *ΔyfiN.* In M9 glucose, however,
292 both strains grew similarly, and the early lag seen in M9 glycerol for WT was not observed
293 (**Fig. 6B**). To test whether this observation was strain specific, we repeated the same
294 experiment using WT and isogenic *ΔyfiN* derivatives of the uropathogenic *E. coli* strain
295 CFT073. The longer lag pattern seen for our WT strain (MG1655) in glycerol (**Fig. 6A**), was
296 also seen for CFT073 compared to its *ΔyfiN* counterpart (**Fig. S8).**

297 To test if the antibiotic tolerance seen during growth delay/arrest by ectopic expression

298 of YfiN (**Fig. 5**) would also be seen under native conditions where growth of the WT strain was
299 delayed (**Fig. 6A**), we sampled aliquots of the YfN +/- strains at 2, 3, and 4 hour (which fall
300 within the time windows monitored in **Fig. 6A/B**), and measured their ability to survive a 4-
301 hour exposure to Ampicillin. The survival data for the WT strain inoculated in either glycerol
302 for glucose could be superimposed on growth periods that coincided with the extended lag for
303 the WT strain (**Fig. 6AB**) i.e. WT survived better than Δ*yfiN* after antibiotic treatment only
304 during the lag phase and only in M9M (compare **Fig. 6C** and **Fig. 6D).** The larger killing effect
305 of Ampicillin on the strains grown on glucose could be due to the reported enhanced killing on
306 this metabolite [47, 48].

307 If the lag was due to a burst of YfiN synthesis as reported [46], this should be reflected
308 in c-di-GMP levels. These were monitored by the riboswitch sensor at the same time points
309 where antibiotic survival was measured i.e. 2, 3 and 4 hour. The data are plotted as a ratio of
310 c-di-GMP in WT vs Δ*yfiN* (**Fig. S9**). Compared to Δ*yfiN,* the WT strain shows higher c-di-GMP
311 levels at 2 and 3 hour but not at 4 hour, mirroring the antibiotic survival pattern in **Fig. 6C**.

312 In summary, the growth delay/arrest property of YfiN is seen even when the protein is
313 expressed from its native chromosomal location, and is not an artifact of ectopic expression.

314

315 ## Discussion

316 C-di-GMP is the most ubiquitous signaling nucleotide in bacteria, with dozens of DGCs
317 involved in its production. These enzymes enable a variety of downstream outputs. In this
318 study, we have discovered a new output for the DGC YfiN, made possible by a particular
319 structural feature of the enzyme that restricts growth in specific nutrient conditions, allowing *E.*
320 *coli* to survive through stressors like antibiotics.

321 **YfiN exploits the absence of autoinhibitory I sites to enable a novel mode of survival**

322 I sites (I_p-I_s) are common in DGCs, and serve an important role in binding c-di-GMP to feed-
323 back regulate DGC activity [12, 20], thus controlling the amount of c-di-GMP available to bind
324 to downstream effector proteins. YfiN belongs to a small fraction of DGCs in *E. coli* (3/12,
325 based on sequence gazing) that do not encode these sites. Absence of this regulatory
326 structural feature appears to be the hallmark of the majority (>90%) of all bacterial YfiN
327 homologs found in the UniProt database. YfiN activity is instead controlled by the periplasmic
328 repressor YfiR, known to be inactivated by redox stress [16, 24]. Given that YfiN is the most
329 robust DGC in *E. coli* [24], we suspect other periplasmic stresses that unfold proteins may
330 also activate this enzyme [49]. Signals that might activate transcription of *yfiN* are still unknown.
331 Once activated, one would not expect YfiN to stop c-di-GMP synthesis until the inducing
332 stressors are gone. We show in this study that unregulated c-di-GMP production comes with
333 a metabolic cost. The nature of this cost came to the fore when *E. coli* grown on gluconeogenic
334 carbon sources such as glycerol, mannitol, or sorbitol were observed to arrest cell growth, a
335 phenotype that required the DGC activity of YfiN (**Fig. 1**), but did not require its relocation to
336 the cell division site at the mid-cell (**Fig. 2**). That it was the unregulated DGC activity of YfiN
337 that was responsible for growth arrest was established by reconstituting the consensus
338 sequence of both I_p and I_s sites, which restored growth (**Fig. 3C**). Conversely, inactivating the
339 I_p site of DgcA from *C. cresentus*, conferred on it the growth arrest phenotype (**Fig. 3E**).

340 The studies described above were performed under ectopic expression of YfiN alone,
341 in order to mimic conditions where YfiR is non-functional. Deleting *yfiR* was not sufficient to
342 induce growth arrest from the native levels of YfiN. While we do not as yet know which
343 environmental signals might activate *yfiN* expression, a brief spike in YfiN levels was reported
344 when an overnight culture of *E. coli* was inoculated into fresh media [46]. As discussed below,
345 we have leveraged this finding to show that during this brief spike, native YfiN recapitulates
346 the data from ectopic expression. We imagine that in natural habitats, a combination of
347 periplasmic stress plus the stress of growing on energetically costly substrates, combined

348 perhaps with environmental signals that activate *yfiN* transcription, might create fertile grounds
349 for growth arrest. That this arrest is reversible, as seen by revival of growth upon adding non-
350 gluconeogenic sugars (**Fig. S2E**), suggests that *E. coli* employs YfiN to weather inhospitable
351 conditions. A reversible quiescent state is known to favor adaptive evolution from microbes to
352 humans [50-52]. Our findings likely extend to all YfiN-encoding bacteria given that the majority
353 of the homologs lack the I_p site. In those that do have this site (*Pseudomonas* and *Yersinia*
354 species), the I_s site is absent (**Fig. S10**). In light of our data showing that both I sites are
355 required to relieve growth arrest (**Fig. 3C**), feed-back inhibition of YfiN activity is likely
356 inefficient in the bacteria harboring only the I_p site [21, 22].

357 **YfiN activity during growth on gluconeogenic carbon sources depletes cellular GTP**

358 The clear distinction between gluconeogenic and glycolytic carbon sources in promoting
359 growth arrest by YfiN is striking (**Fig. 1D**). Gluconeogenesis is the process by which cells
360 synthesize glucose 6-phosphate from non-hexose sugars [53]. While eukaryotic cells as well
361 as other bacteria consume both ATP and GTP in this process, *E. coli* is known to only consume
362 ATP [54]. Each cycle of gluconeogenesis requires 4 ATPs plus 2 NADHs, resulting in net deficit
363 of 9 ATPs. Lower levels of ATP will consequently lower those of GTP, since the γ phosphate
364 of ATP is used by nucleoside diphosphate kinase (ndk) to synthesize GTP from GDP [55] (**Fig.
365 7**). In glycerol, there is less ATP produced during TCA cycle as well (20 ATPs compared to
366 36~38 ATPs in glucose). Indeed, *E. coli* grown in M9 glycerol and acetate has been
367 demonstrated to have less intracellular ATP/GTP than in glucose [43]. Unregulated
368 consumption of GTP by YfiN will further increase cellular metabolic stress under these
369 conditions. The lower cellular GTP levels we see upon induction of YfiN during growth on M9M
370 are therefore expected (**Fig. 4A**). Lowering GTP levels even by two-fold (**Fig. 4B,C,F**) should
371 be sufficient to arrest growth given *in vitro* data showing that the transcription rate from a
372 ribosomal RNA promoter (*rrnB*) is highly sensitive to GTP concentrations [56]. It was reported
373 earlier that depletion of intracellular GTP by 50% along with decrease in ATP levels, by

374 overexpression of RelA homologues contributes to persister formation by arresting cell growth
375 [57]. In eukaryotes, cancer drugs that cause similar drop in GTP levels resulted in cell death
376 in a human cancer cell line [58]. In the ecological niches that heterotrophic bacteria inhabit,
377 they obtain carbon from dissolved organic matter. Although *E. coli* is primarily a commensal of
378 mammals, and to a lesser extent birds, it can be isolated from a variety of host species as well
379 as soil, sediments, and water. We imagine that the particular YfiN function we have uncovered
380 in this study may manifest in certain ecological niches rich in gluconeogenic sugars or in non-
381 carbohydrate substrates not tested in this study. For example, each part of the human gut has
382 different concentrations of carbon sources and types [59].

383 In summary, we conclude that uncontrolled synthesis of c-di-GMP by YfiN is the
384 proximate cause of depletion of cellular GTP. These nucleotides are essential for the synthesis
385 of the major cellular macromolecules DNA, RNA and protein, explaining why cells enter growth
386 arrest when using the energetically more costly gluconeogenic carbon sources for synthesis
387 of glucose-6-P.

388 **YfiN contributes to increased tolerance to antibiotics**

389 YfiN is known to inhibit cell division in response to redox and envelope stresses, and to protect
390 *E. coli* from envelope-disrupting environments when ectopically expressed [24]. We show here
391 that ectopic expression of YfiN in M9M also increases tolerance to a broad class of antibiotics
392 such as Ampicillin, Gentamicin, and Ciprofloxacin, which target and disrupt a variety of cellular
393 processes (**Fig. 5**). This is a result of YfiN's unregulated DGC activity (**Fig. 1C, 3C**). Bacteria
394 are continuously exposed to environmental stresses and knowing when to stop proliferating is
395 key to their survival. Our finding that transferring *E. coli* cells from a stationary culture to M9
396 glycerol delays growth by extending the lag phase (**Fig. 6AB)**, might suggest that transitioning
397 from one nutritional environment to another is one such stress that activates YfiN expression
398 [46]. The growth delay upon transitioning from LB to M9M is accompanied by increased c-di-

399 GMP levels (**Fig. S9**), and increased tolerance to antibiotics compared to a Δ*yfiN* strain (**Fig.**
400 **6C**). This result is similar to antibiotic tolerance observed when cell growth is delayed/arrested
401 by ectopic expression of YfIN. Although it may seem counter-intuitive to harbor a gene
402 preventing bacteria from proliferating, persisting in the lag phase may help bacteria in
403 transitioning to the new environment, particularly if the environment is stressful or nutrients
404 are scarce. An increase in the lag phase has been reported as an integral step for developing
405 antibiotic resistance [60, 61]. It has been suggested that a prolonged lag could buy the bacteria
406 time to diversify adaptive phenotypes [62, 63]. The importance of the lag phase is not limited
407 to surviving antibiotic stress alone. A transcriptional profiling study of *S. enterica* showed that
408 genes associated with DNA repair and protein degradation were induced during lag phase,
409 implicating a crucial role for this phase in repairing damaged cellular components [61, 64].
410 Bacteria are also known to reorganize their metabolism during the lag phase to achieve
411 optimal growth [64], and two distinct lag phases were observed in *E. coli* supplied with
412 arabinose [65]. Thus, by regulating the duration of the lag phase, we suspect that YfiN not
413 only confers increased tolerance to antibiotics but also other advantages such as optimizing
414 DNA repair and metabolic pathways for growth.

415

416 **Coda**. YfiN seems to have emerged as a DGC that responds to multiple metabolic stresses –
417 redox, envelope, gluconeogenic substrates – and has thus far shown multiple output
418 responses designed to hunker down, make biofilms, and persist.

419

420 **Acknowledgements**

421 We thank Y. Fitnat, HK. Kim and S. Bhattacharyya for strains and for helpful discussions. This
422 work was supported by NIH grant R35GM118085.

423 ## Materials and Methods

424 **Strains, growth conditions, mutagenesis, and plasmid constructions**. Strains and
425 plasmids used in this study are listed in Table S1. The WT parent strain for *E. coli* was MG1655
426 for all experiments. All strains were grown in M9M (M9 minimal media + 0.2% glycerol + 0.2%
427 casamino acid) or in LB broth (10 g/liter tryptone, 5 g/liter yeast extract, 5 g/liter NaCl) unless
428 noted otherwise. When appropriate, the following antibiotics were used: Ampicillin (100 μg/ml),
429 Chloramphenicol (20 μg/ml), Kanamycin (50 μg/ml), and Gentamicin (30 μg/ml). For inducible
430 plasmids, 100μM isopropyl-β-d-thiogalactopyranoside (IPTG) or 0.02%(w/v) L-arabinose were
431 added as indicated in the figures or legends. To monitor the growth of cells, optical density
432 was measured at the wavelength of 600nm (OD_{600})

433 HK 533 strain was constructed similarly to HK532 strain [24]. Using lambda red recombination
434 [66], *yfiR* was replaced with PTrc promoter and a kanamycin cassette inserted in an orientation
435 opposite to the direction (←) of *yfi* operon transcription, in order to prevent polar effects on
436 *yfiN* expression.

437 For cloning of expression plasmids, gene sequences were amplified from the genomic DNA
438 of WT strains by using PCR and introduced into pBAD30, pBAD33.

439 To restore or introduce I-sites, specific primers designed for single base pair substitutions were
440 used for PCR amplification using pBAD_YfiN or DgcA as templates. Following amplification,
441 the original templates were digested with 1 unit of DpnI and PCR products were used for
442 transformation and selection. All constructs were confirmed by DNA sequencing.

443 **Recovery assay.** For the experiment shown in Fig. S2E, cYfiN strain was propagated in M9M
444 with IPTG for induction. After 2 hours post-induction, 0.2% glucose was added for recovery,
445 followed by measurement of OD_{600} every 2 hours.

446 **Motility assay.** LB soft agar or swim plates were made using 0.3% Fisher agar. 5 μl of an

447 overnight culture was inoculated in the center and plates incubated at 30°C for 8-12 hours.
448 Swim ring diameter was measured to compare motility across strains.

449 **Biofilm assay.** Cells were propagated in M9M in 96-well plates. After 20-hour incubation at
450 37℃, plates were washed twice with water and dried for 2 hours at RT. 125μl of 0.01% Crystal
451 violet solution (w/v) was added to each well and incubated in RT for 15 min. The plate was re-
452 washed three times with water and then 125μl 30% Acetic acid (v/v) were added to each well.
453 After 15 min incubation in RT, solutions in each well were transferred to a new 96 well plate.
454 O.D. 550nm was used to measure biofilm formation, and OD_{600} for data normalization.

455 **Fluorescence microscopy**. Overnight cultures of cells with plasmids encoding fluorescent
456 fusion proteins were diluted 1:100 in fresh M9M or LB medium with antibiotics and grown at
457 30°C with 0.02% arabinose for 4 hours (unless otherwise stated). For imaging cells, a cell
458 suspension (5 μl) was applied to a slide and incubated for 5 min before imaging. Images were
459 acquired using an Olympus BX53 microscope, appropriate filters, and cellSens standard
460 software (version 1.6) from Olympus.

461 **Western Blot**. Overnight cultures of cells with plasmids encoding YfiN and its mutants (I_{ps},
462 R260A, GGAAF) were diluted 1:100 in M9M and propagated with 0.02% arabinose for 3 hours.
463 Cells were collected and then re-suspended in a lysis buffer with a final concentration of
464 2.5x10^9/ml cells. Upon cell lysis using a heat block (100℃), 1x10^7 cells were loaded into
465 each lane on a SDS-gel. Proteins were then transferred to a nitrocellulose membrane and
466 blocked with 5% non-fat dry milk (NFDM) in Tris-buffered saline with 20% Tween (TBST) for 1
467 hour. The membrane was incubated overnight with a 1:1000 dilution of either GFP antibody
468 (Sigma) or FLAG antibody (Sigma Monoclonal FLAG antibody M2) in TBST with 5% NFDM
469 (w/v), and then washed 3 times with TBST every 10 minute intervals. This step was followed
470 immediately by an hour incubation with 1:5000 dilution of Goat α-mouse-HRP (Bio-Rad) in

471 TBST. ECL Select (Amersham; chemiluminescence) was used for a development and the blot
472 image was taken using ChemiDoc (G:BOX).

473 ImageJ software was used to measure the difference in pixel intensities to compare the
474 difference in the levels of expression.

475 **c-di-GMP biosensor assay**. Overnight cultures of cells with plasmids encoding YfiN and
476 riboswitch-based c-di-GMP biosensor ere diluted (1:100) and then propagated in M9M media
477 with an addition of 0.02% arabinose for induction. After a 3-hour incubation, cells were
478 transferred to a 96-well plate (100µl/well). Riboswitches (bc3,4,5) that are situated upstream
479 of *turborfp* (encoding a more photo-stable RFP variant) are activated upon binding of c-di-
480 GMP and allow for downstream gene expression, while *amcyan,* an enhanced CFP variant, is
481 expressed constitutively. Samples were diluted to OD_{600} prior to measurement and the ratio of
482 RFP/CFP was used to estimate c-di-GMP concentration/cell. Excitation/Emission wavelengths
483 of 405/488nm and 553/574nm were used for *amcyan* and *turborfp* respectively using a
484 FlexStation3 Plate Reader.

485 **Gene alignment for identification of primary and secondary I-sites.** Primary I-site
486 designation for YfiN was based on the identified consensus RxxD, situated five amino acids
487 upstream of the GGDEF catalytic site [12, 19, 67]. Secondary I-site designation for YfiN was
488 predicted by comparing sequences from other DGCs that harbor experimentally identified
489 secondary sites. Clustal Omega, available online (https://www.ebi.ac.uk/), was used for the
490 prediction and alignment; DgcA was excluded from the analysis, because it has two predicted
491 secondary I-sites.

492 For analysis of YfiN homologues, we used YfiN protein sequence of *E. coli* MG1655 from the
493 UnitProt database (http://www.uniprot.org; accession number: P46139). Using UniRef50, we
494 acquired 1974 orthologous sequences with minimum 50% sequence identity. Conservation of
495 primary and secondary I-sites was calculated using the Clustal Omega tool.

496 **Antibiotic survival assay on plates.** An overnight culture of cYfiN strain was diluted 1:100
497 in M9M with or without IPTG. After 6 hours post-induction, cells were spread on agar plates
498 containing either Ampicillin (20, 100 μg/ml), Gentamicin (10, 20 μg/ml) or Ciprofloxacin (1,
499 5μg/ml). After 12 hour incubation on these plates, cells were re-spread on fresh LB agar plates
500 without antibiotics.

501 **Antibiotic survival assay in liquid.** An overnight culture of cYfiN strain was inoculated at
502 1:100 dilution in M9M. Cell cultures were grown for 2 hours to reach the OD_{600} of 0.1, at which
503 IPTG was added. Two hours post-induction, either Gentamicin (20 μg/ml) or Ciprofloxacin
504 (10μg/ml) was added. After a 4 hour treatment with antibiotics, cell cultures were washed with
505 PBS (phosphate buffered saline) buffer twice and plated on LB agar for CFU counts. The
506 percent survival was calculated as follows: (final CFU/CFU before antibiotic treatment) × 100.
507 The results are presented as the average results from at least 3 biological replicates.

508 **Thin layer chromatography assay** YfiN, YfiN I-site mutants (I_p, I_s, I_{ps}), and DgcA were
509 induced from pBAD plasmids with arabinose in M9M for 3 hours. Then, cells were washed
510 twice with PBS buffer and lysed with a VCX-750 Vibra-Cell sonicator at 20kHz (30 sec pulse
511 followed by 10 sec cool-down for total of 5 cycles). Cell lysates were incubated with 1 mM
512 GTP/[α-^{32}P]GTP (0.1 μCi/μl) (PerkinElmer) and incubated at 30°C for various time intervals
513 for comparison pYfiN and pYfiN(Ips). Reactions were stopped by the addition of 1 volume of
514 0.5 M EDTA. Radio-labeled products were analyzed by polyethyleneimine-cellulose thin-layer
515 chromatography (TLC; Millipore), by spotting 2 μl samples onto TLC plates. Plates were dried
516 at RT for 5 min, and developed in 1.3 M KH_2PO_4 (pH 3.2) [12]. TLC data was analyzed with
517 GE Typhoon Phosphorimager and ImageJ software by comparing the intensities of each blots
518 on the TLC plate. GTP consumption was estimated based on the input GTP concentration.

519 **GTPase assay.** The GTP levels were measured using a GTPase-Glo Assay kit (Promega)
520 which employs an ATP-linked luciferase reaction. Total concentration of GTP in cells was

521 calculated based on the standard curve generated using a standard provided by manufacturer,
522 and normalized to OD_{600} (OD_{600} 1.0 = 5x10^8 cells). The final concentration was represented
523 in ng/cell.

524 **Metabolomics**. *E. coli* MG1655 yfiR::kan pTrc99a-$YfiN_{GFP}$ (HK533) was grown at 30°C for 2
525 hours in 10 ml M9M, with IPTG for induction. Cells were incubated for additional 3 hours post-
526 induction (OD_{600} reached around 0.4). Pellets were collected and flash frozen. They were
527 shipped on dry ice to the Metabolomics Core Facility at the Mayo Clinic at Rochester, which
528 routinely analyzes a panel of 219 commonly investigated metabolites such as dNTPs, NTPs,
529 carbohydrates, and acids. We provided them with c-di-GMP, and they estimated these
530 concentrations [68]. Samples were analyzed by high-performance liquid chromatography–
531 tandem mass spectrometry (HPLC-MS/MS) at the facility, using a Thermo Fisher Q Exactive
532 mass spectrometer. The analysis is qualitative, and data are provided as areas under elution
533 peaks (AU, arbitrary unit). Of the 3 biological replicates (each with two technical replicate) sent
534 to the Facility, one was unusable. COVID-19 work protocols during this time (August to
535 November, 2020), prevented us from sending more samples.

536 Absolute quantification of the targeted nucleotides c-di-GMP and rNTPs was done by (HPLC-
537 MS/MS) at the Metabolomics Core Facility at the University of Texas Medical Branch (UTMB).
538 Cells were grown in M9M except with arabinose for induction. After 3.5 hours post-induction,
539 cells were collected and their wet weight was measured for data normalization. Pellets were
540 then flash frozen and mailed to UTMB. Three biological replicates for each set consisting
541 $_p$Empty, $_p$YfiN, $_p$YfiN(I_{ps}), $_p$DgcA were prepared. The facility used ^{13}C-labeled standards to
542 obtain a standard curve against which experimental values were derived.

543 **Growth rate calculation.** Strains grown in M9M were collected at 0, 2, 4, and 6 hours for
544 counting CFUs. Growth rate h^{-1} = (CFU_{final}/$CFU_{initial}$)/2.

545 ## References

546 1. Galperin, M.Y., *Bacterial signal transduction network in a genomic perspective.* Environmental
547 microbiology, 2004. **6**(6): p. 552-567.
548 2. Francis, V.I. and S.L. Porter, *Multikinase Networks: Two-Component Signaling Networks*
549 *Integrating Multiple Stimuli.* Annual Review of Microbiology, 2019. **73**(1): p. 199-223.
550 3. Boor, K.J., *Bacterial stress responses: what doesn't kill them can make then stronger.* PLoS
551 biology, 2006. **4**(1): p. e23-e23.
552 4. Fang, F.C., et al., *Bacterial Stress Responses during Host Infection.* Cell host & microbe, 2016.
553 **20**(2): p. 133-143.
554 5. Ross, P., et al., *Regulation of cellulose synthesis in Acetobacter xylinum by cyclic diguanylic*
555 *acid.* Nature, 1987. **325**(6101): p. 279-281.
556 6. Römling, U., M.Y. Galperin, and M. Gomelsky, *Cyclic di-GMP: the first 25 years of a universal*
557 *bacterial second messenger.* Microbiology and molecular biology reviews : MMBR, 2013.
558 **77**(1): p. 1-52.
559 7. Jenal, U., A. Reinders, and C. Lori, *Cyclic di-GMP: second messenger extraordinaire.* Nature
560 Reviews Microbiology, 2017. **15**(5): p. 271-284.
561 8. Lori, C., et al., *Cyclic di-GMP acts as a cell cycle oscillator to drive chromosome replication.*
562 Nature, 2015. **523**(7559): p. 236-239.
563 9. Tamayo, R., J.T. Pratt, and A. Camilli, *Roles of cyclic diguanylate in the regulation of bacterial*
564 *pathogenesis.* Annual review of microbiology, 2007. **61**: p. 131-148.
565 10. Hoffman, L.R., et al., *Aminoglycoside antibiotics induce bacterial biofilm formation.* Nature,
566 2005. **436**(7054): p. 1171-5.
567 11. Suchanek, V.M., et al., *Chemotaxis and cyclic-di-GMP signalling control surface attachment*
568 *of Escherichia coli.* Mol Microbiol, 2020. **113**(4): p. 728-739.
569 12. Christen, B., et al., *Allosteric Control of Cyclic di-GMP Signaling.* Journal of Biological
570 Chemistry, 2006. **281**(42): p. 32015-32024.
571 13. Orr, M.W., et al., *A Subset of Exoribonucleases Serve as Degradative Enzymes for pGpG in*
572 *c-di-GMP Signaling.* Journal of Bacteriology, 2018. **200**(24): p. e00300-18.
573 14. Hasegawa, K., S. Masuda, and T.-a. Ono, *Light Induced Structural Changes of a Full-length*
574 *Protein and Its BLUF Domain in YcgF(Blrp), a Blue-Light Sensing Protein That Uses FAD*
575 *(BLUF).* Biochemistry, 2006. **45**(11): p. 3785-3793.
576 15. Tuckerman, J.R., et al., *An oxygen-sensing diguanylate cyclase and phosphodiesterase couple*
577 *for c-di-GMP control.* Biochemistry, 2009. **48**(41): p. 9764-74.
578 16. Jacob G. Malone , T.J., Pablo Manfredi,Andreas Dötsch,Andrea Blanka,Raphael Bos,Guy R.
579 Cornelis,Susanne Häussler,Urs Jenal *The YfiBNR Signal Transduction Mechanism Reveals*
580 *Novel Targets for the Evolution of Persistent Pseudomonas aeruginosa in Cystic Fibrosis*
581 *Airways.* PLOS PATHOGENS, 2012. **8(6): e1002760.**

582 17. Walker, J.A., S. Rivera, and E.E. Weinert, *Mechanism and Role of Globin-Coupled Sensor*
583 *Signalling.* Advances in microbial physiology, 2017. **71**: p. 133-169.
584 18. Zähringer, F., et al., *Structure and Signaling Mechanism of a Zinc-Sensory Diguanylate*
585 *Cyclase.* Structure, 2013. **21**(7): p. 1149-1157.
586 19. Wassmann, P., et al., *Structure of BeF3- -modified response regulator PleD: implications for*
587 *diguanylate cyclase activation, catalysis, and feedback inhibition.* Structure, 2007. **15**(8): p.
588 915-27.
589 20. Dahlstrom, K.M., et al., *The Inhibitory Site of a Diguanylate Cyclase Is a Necessary Element*
590 *for Interaction and Signaling with an Effector Protein.* J Bacteriol, 2016. **198**(11): p. 1595-
591 603.
592 21. Giardina G, P.A., Fernicola S, Franceschini S, Rinaldo S, Stelitano V, *Investigating the Allosteric*
593 *Regulation of YfiN from Pseudomonas aeruginosa: Clues from the Structure of the Catalytic*
594 *Domain.* PLoS ONE, 2013. **8(11): e81324**.
595 22. Ueda, A. and T.K. Wood, *Tyrosine Phosphatase TpbA of Pseudomonas aeruginosa Controls*
596 *Extracellular DNA via Cyclic Diguanylic Acid Concentrations.* Environ Microbiol, 2010. **2**(3): p.
597 449-55.
598 23. Jacob G. Malone , T.J., Christian Spangler,Daniel Ritz,Anne Spang,Cécile
599 Arrieumerlou,Volkhard Kaever,Regine Landmann,Urs Jenal, *YfiBNR Mediates Cyclic di-GMP*
600 *Dependent Small Colony Variant Formation and Persistence in Pseudomonas aeruginosa.*
601 PLOS PATHOGENS, 2010. **6(3): e1000804**.
602 24. Kim, H.K. and R.M. Harshey, *A Diguanylate Cyclase Acts as a Cell Division Inhibitor in a Two-*
603 *Step Response to Reductive and Envelope Stresses.* mBio, 2016. **7**(4): p. e00822-16.
604 25. Katharios-Lanwermeyer, S., et al., *The Diguanylate Cyclase YfiN of Pseudomonas aeruginosa*
605 *Regulates Biofilm Maintenance in Response to Peroxide.* J Bacteriol, 2022. **204**(1): p.
606 e0039621.
607 26. Egan, A.J. and W. Vollmer, *The physiology of bacterial cell division.* Ann N Y Acad Sci, 2013.
608 **1277**: p. 8-28.
609 27. Hengge, R., et al., *Systematic Nomenclature for GGDEF and EAL Domain-Containing Cyclic*
610 *Di-GMP Turnover Proteins of Escherichia coli.* Journal of bacteriology, 2015. **198**(1): p. 7-11.
611 28. Richter, A.M., et al., *Local c-di-GMP Signaling in the Control of Synthesis of the E. coli Biofilm*
612 *Exopolysaccharide pEtN-Cellulose.* J Mol Biol, 2020. **432**(16): p. 4576-4595.
613 29. Pfiffer, V., et al., *Genetic dissection of Escherichia coli's master diguanylate cyclase DgcE: Role*
614 *of the N-terminal MASE1 domain and direct signal input from a GTPase partner system.*
615 PLOS Genetics, 2019. **15**(4): p. e1008059.
616 30. Junkermeier, E.H. and R. Hengge, *A Novel Locally c-di-GMP-Controlled Exopolysaccharide*
617 *Synthase Required for Bacteriophage N4 Infection of Escherichia coli.* mBio, 2021. **12**(6): p.
618 e0324921.
619 31. Frankel, D., *Glycolysis*. Escherichia coli and Salmonella tiphymurium: Cellular and Molecular

Biology. 2.

, ed. F. Neidhardt. 1996. 189–196.

32. Nieto, V., et al., *Under Elevated c-di-GMP in Escherichia coli, YcgR Alters Flagellar Motor Bias and Speed Sequentially, with Additional Negative Control of the Flagellar Regulon via the Adaptor Protein RssB.* Journal of Bacteriology, 2019. **202**(1): p. e00578-19.
33. Zhou, H., et al., *Characterization of a natural triple-tandem c-di-GMP riboswitch and application of the riboswitch-based dual-fluorescence reporter.* Sci Rep, 2016. **6**: p. 20871.
34. Floyd, K.A., et al., *c-di-GMP modulates type IV MSHA pilus retraction and surface attachment in Vibrio cholerae.* Nature Communications, 2020. **11**(1): p. 1549.
35. Chan, C., et al., *Structural basis of activity and allosteric control of diguanylate cyclase.* Proc Natl Acad Sci U S A, 2004. **101**(49): p. 17084-9.
36. Hauryliuk, V., et al., *Recent functional insights into the role of (p)ppGpp in bacterial physiology.* Nature reviews. Microbiology, 2015. **13**(5): p. 298-309.
37. Diehl, F.F., et al., *Cellular redox state constrains serine synthesis and nucleotide production to impact cell proliferation.* Nature Metabolism, 2019. **1**(9): p. 861-867.
38. Diehl, F.F., et al., *Nucleotide imbalance decouples cell growth from cell proliferation.* Nature Cell Biology, 2022. **24**(8): p. 1252-1264.
39. Patil, P.R., et al., *A revised mechanism for (p)ppGpp synthesis by Rel proteins: The critical role of the 2'-OH of GTP.* J Biol Chem, 2020. **295**(37): p. 12851-12867.
40. Kriel, A., et al., *Direct regulation of GTP homeostasis by (p)ppGpp: a critical component of viability and stress resistance.* Molecular cell, 2012. **48**(2): p. 231-241.
41. Gaca, A.O., C. Colomer-Winter, and J.A. Lemos, *Many means to a common end: the intricacies of (p)ppGpp metabolism and its control of bacterial homeostasis.* Journal of bacteriology, 2015. **197**(7): p. 1146-1156.
42. Ronneau, S. and R. Hallez, *Make and break the alarmone: regulation of (p)ppGpp synthetase/hydrolase enzymes in bacteria.* FEMS Microbiology Reviews, 2019. **43**(4): p. 389-400.
43. Bennett, B.D., et al., *Absolute metabolite concentrations and implied enzyme active site occupancy in Escherichia coli.* Nature chemical biology, 2009. **5**(8): p. 593-599.
44. Granner, D. and S. Pilkis, *The genes of hepatic glucose metabolism.* J Biol Chem, 1990. **265**(18): p. 10173-6.
45. Kohanski, M.A., D.J. Dwyer, and J.J. Collins, *How antibiotics kill bacteria: from targets to networks.* Nature reviews. Microbiology, 2010. **8**(6): p. 423-435.
46. Sarenko, O., et al., *More than Enzymes That Make or Break Cyclic Di-GMP—Local Signaling in the Interactome of GGDEF/EAL Domain Proteins of Escherichia coli.* mBio, 2017. **8**(5): p. e01639-17.

47. Allison, K.R., M.P. Brynildsen, and J.J. Collins, *Metabolite-enabled eradication of bacterial persisters by aminoglycosides.* Nature, 2011. **473**(7346): p. 216-20.
48. Prax, M., et al., *Glucose Augments Killing Efficiency of Daptomycin Challenged Staphylococcus aureus Persisters.* PLOS ONE, 2016. **11**(3): p. e0150907.
49. Mitchell, A.M. and T.J. Silhavy, *Envelope stress responses: balancing damage repair and toxicity.* Nat Rev Microbiol, 2019. **17**(7): p. 417-428.
50. Gresham D, D.M., Tucker CM, Jenq HT, Pai DA, Ward, *A The Repertoire and Dynamics of Evolutionary Adaptations to Controlled Nutrient-Limited Environments in Yeast.* PLoS Genetics, 2008. **4(12): e1000303.** https://doi.org/10.1371/journal.pgen.1000303.
51. Daignan-Fornier B, L.D.a.S., *Quiescence Through the Prism of Evolution.* Front. Cell Dev. Biol, 2021. **9:745069**(10.3389/fcell.2021.745069).
52. Moore, N. and S. Lyle, *Quiescent, slow-cycling stem cell populations in cancer: a review of the evidence and discussion of significance.* J Oncol, 2011. **2011**.
53. Tchawa Yimga, M., et al., *Role of gluconeogenesis and the tricarboxylic acid cycle in the virulence of Salmonella enterica serovar Typhimurium in BALB/c mice.* Infect Immun, 2006. **74**(2): p. 1130-40.
54. Sauer, U. and B.J. Eikmanns, *The PEP—pyruvate—oxaloacetate node as the switch point for carbon flux distribution in bacteria: We dedicate this paper to Rudolf K. Thauer, Director of the Max-Planck-Institute for Terrestrial Microbiology in Marburg, Germany, on the occasion of his 65th birthday.* FEMS Microbiology Reviews, 2005. **29**(4): p. 765-794.
55. Kuroda, A. and A. Kornberg, *Polyphosphate kinase as a nucleoside diphosphate kinase in Escherichia coli and Pseudomonas aeruginosa.* Proceedings of the National Academy of Sciences, 1997. **94**(2): p. 439-442.
56. Gaal, T., et al., *Transcription Regulation by Initiating NTP Concentration: rRNA Synthesis in Bacteria.* Science, 1997. **278**(5346): p. 2092.
57. Jimmy, S., et al., *A widespread toxin−antitoxin system exploiting growth control via alarmone signaling.* Proceedings of the National Academy of Sciences, 2020. **117**(19): p. 10500-10510.
58. Li, G., et al., *Prolonged depletion of guanosine triphosphate induces death of insulin-secreting cells by apoptosis.* Endocrinology, 1998. **139**(9): p. 3752-62.
59. Visconti, A., et al., *Interplay between the human gut microbiome and host metabolism.* Nature Communications, 2019. **10**(1): p. 4505.
60. Fridman, O., et al., *Optimization of lag time underlies antibiotic tolerance in evolved bacterial populations.* Nature, 2014. **513**(7518): p. 418-421.
61. Bertrand, R.L., *Lag Phase Is a Dynamic, Organized, Adaptive, and Evolvable Period That Prepares Bacteria for Cell Division.* Journal of Bacteriology, 2019. **201**(7): p. e00697-18.
62. Sánchez-Romero, M.A. and J. Casadesús, *Contribution of phenotypic heterogeneity to adaptive antibiotic resistance.* Proceedings of the National Academy of Sciences, 2014. **111**(1): p. 355-360.

696 63. Adkar, B.V., et al., *Optimization of lag phase shapes the evolution of a bacterial enzyme.*
697 Nature Ecology & Evolution, 2017. **1**(6): p. 0149.
698 64. Rolfe, M.D., et al., *Lag phase is a distinct growth phase that prepares bacteria for exponential*
699 *growth and involves transient metal accumulation.* J Bacteriol, 2012. **194**(3): p. 686-701.
700 65. Madar, D., et al., *Promoter activity dynamics in the lag phase of Escherichia coli.* BMC Syst
701 Biol, 2013. **7**: p. 136.
702 66. Datsenko, K.A. and B.L. Wanner, *One-step inactivation of chromosomal genes in Escherichia*
703 *coli K-12 using PCR products.* Proceedings of the National Academy of Sciences, 2000.
704 **97**(12): p. 6640-6645.
705 67. Hengge, R., *Principles of c-di-GMP signalling in bacteria.* Nature Reviews Microbiology, 2009.
706 **7**(4): p. 263-273.
707 68. Spangler, C., et al., *A liquid chromatography-coupled tandem mass spectrometry method*
708 *for quantitation of cyclic di-guanosine monophosphate.* Journal of Microbiological Methods,
709 2010. **81**(3): p. 226-231.
710 69. Amann, E., J. Brosius, and M. Ptashne, *Vectors bearing a hybrid trp-lac promoter useful for*
711 *regulated expression of cloned genes in Escherichia coli.* Gene, 1983. **25**(2-3): p. 167-78.
712 70. Guzman, L.M., et al., *Tight regulation, modulation, and high-level expression by vectors*
713 *containing the arabinose PBAD promoter.* J Bacteriol, 1995. **177**(14): p. 4121-30.

714

715

716

717

718

719

720

721

722

723

724 **Main Figures**

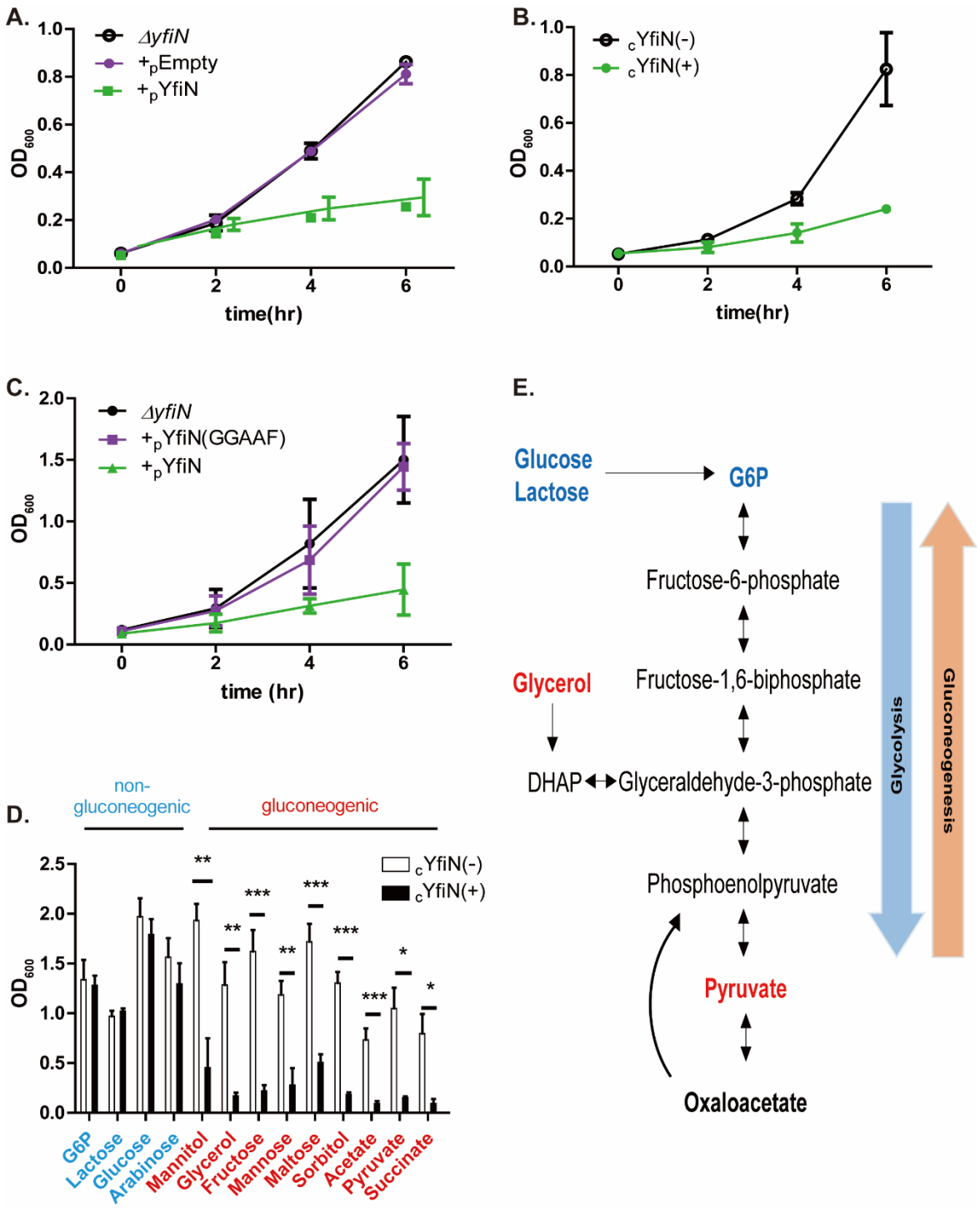

725

726 **Figure 1. YfiN arrests *E. coli* growth only on specific carbon sources.** *(A)* Time course of growth
727 (OD_{600}) in M9M of Δ*yfiN E. coli* harboring either pYfiN or pEmpty (control) plasmids, where expression
728 of *yfiN* is driven from the PBAD promoter (see Methods for media and arabinose inducer concentrations).
729 *(B)* As *(A)*, except *yfiN* expression is from its chromosomal location ($cYfiN_{GFP}$), driven from the PTrc
730 promoter. +/- indicate IPTG addition. *(C)* As in *A*, except activity of pYfiN is compared with its active site

731 mutant YfiN(GGAAF). (*D)* As in *B* (cYfiN)*,* except cells were grown in M9 media supplemented with
732 indicated sugars, and OD_{600} measured at 8h. (*E*) Schematic of the gluconeogenesis and glycolysis
733 pathways, with relevant metabolites color-coded as in *D*. Data in all experiments, here and in the
734 following figures (where applicable), were analyzed with the unpaired t-test, with three biological
735 replicates for each sample, unless noted otherwise. p-value <0.001 ***, <0.01 **, and <0.5 *.

736

737

738

739

740

741

742

743

744

745

746

747

748

749

750

751

752

753

754

755

756

757

758

759

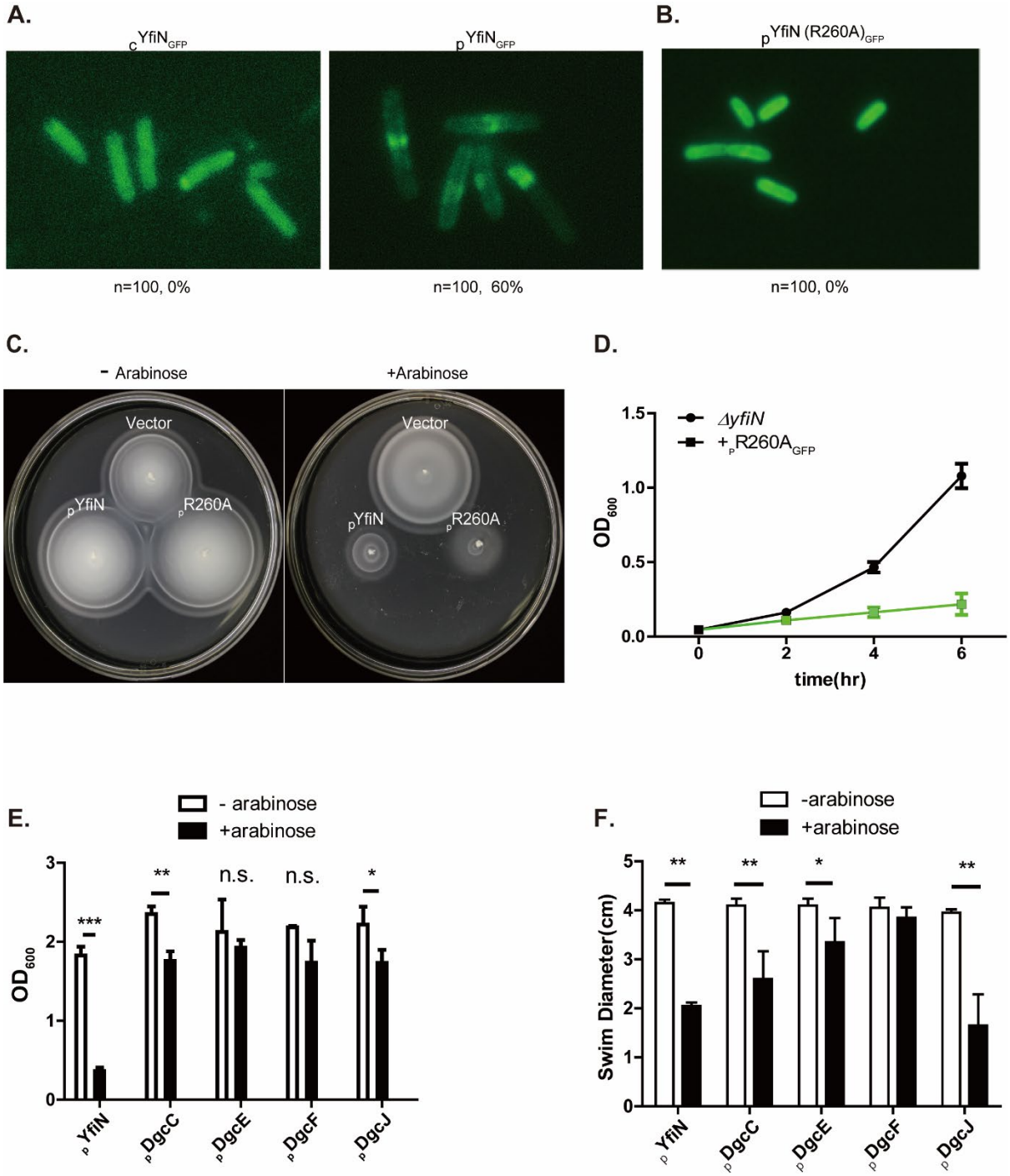

Figure 2. Growth-arrest phenotype of YfiN in M9M is independent of its relocation to the mid-cell. *(A)* Fluorescence images of $cYfiN_{GFP}$ and $pYfiN_{GFP}$ expressed for 4 hours in M9M. The percentage of cells with $YfiN_{GFP}$ foci at the mid-cell is indicated, with n = total number of cells observed. *(B)* As in *A*, except with pYfiN $(R260A)_{GFP}$. *(C)* Motility of indicated strains: empty vector, $_pYfiN_{GFP}$, $_pYfiN(R260A)_{GFP}$, -/+ arabinose inducer in 0.3% soft agar plates. *(D)* As in *C*, except growth curves of the indicated strains in M9M. *(E)* A panel of all five inner membrane DGCs of *E. coli* were cloned in the PBAD vector and expressed for 12 hoursprior to recording OD_{600}. (*F*) Motility assay of strains from *E* in soft agar plates.

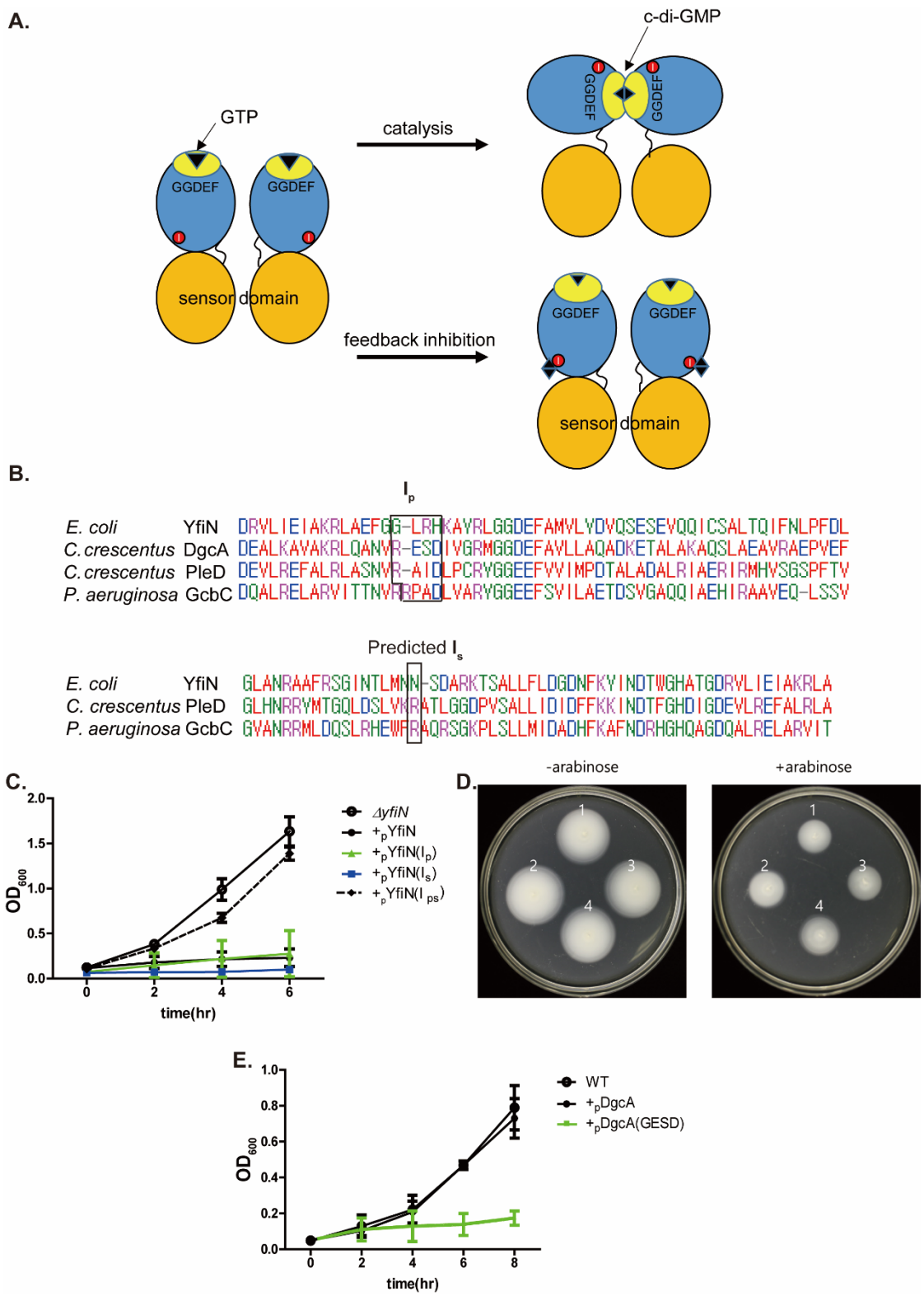

Figure 3. Growth arrest by YfiN is related to absence of autoinhibitory I sites. *(A)* Schematic of I-site mediated feedback inhibition. Dimeric DGCs sense environmental stimuli though their sensor domains (orange), and relay the signal to their catalytic domain (blue) to synthesize c-di-GMP. Upon reception of the sensory signal, GGDEF active sites (yellow) align in the dimer [7] to produce c-di-GMP

774 (diamond) from 2 GTPs. Product inhibition occurs when c-di-GMP binds to I-sites (red circles), preventing
775 the two active sites from interacting. (*B*) The primary (I_p) (RxxD) and predicted secondary (I_s) auto-
776 inhibitory sites are boxed in a sequence alignment of various DGCs around these sites (see Methods).
777 (*C*) Growth in M9M of pYfiN derivatives reconstituted for primary (Ip), secondary (Is) or both (Ips) I-sites.
778 Expression was induced with arabinose. (*D*) Motility of indicated strains (1: pYfiN, 2: pYfiN I_p, 3: pYfiN
779 I_s, 4: pYfiN I_{ps}) assayed in soft agar plates. (*E)* As in C, except with cells expressing DgcA and its mutant
780 I_p site (RESD→GESD).

781

782

783

784

785

786

787

788

789

790

791

792

793

794

795

796

797

798

799

800

801

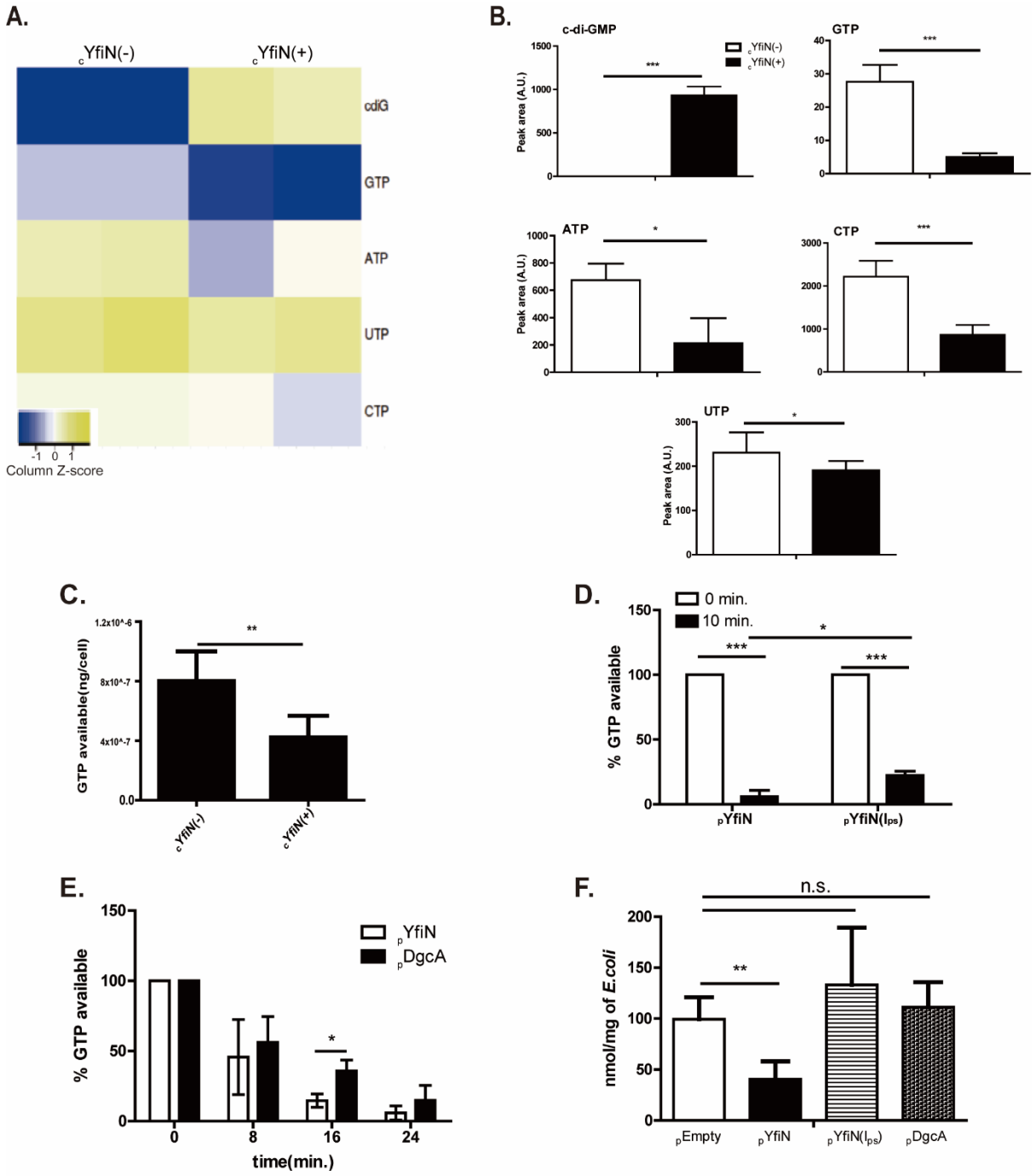

Figure 4. YfiN depletes intracellular GTP. (*A*) Metabolite profiling of cYfIN$_{GFP}$ was performed using two biological replicates (each with 2 technical replicates) with and without inducer (+/-) (see Methods). Among ~219 metabolites measured using the targeted metabolomics approach, levels of c-di-GMP (cdiG) and the four ribonucleotides (GTP, ATP, UTP, CTP) are shown. Peak areas under selected metabolite elution profiles are $\log_{10}$ transformed and displayed as a heatmap, data from each biological replicate (each with two technical replicates) occupying a square. *(B)* To measure the statistical significance of the estimates in A, the areas under the curve of eluted peaks were calibrated as AU (arbitrary units), and the data replotted as bar graphs. (*C*) A luciferase-based GTP assay kit was used to measure GTP levels (ng/cell) in lysates of cYfiN$_{GFP}$-expressing cells 3 hours post-induction. (*D)* Lysates of M9M-grown cells expressing $_p$YfiN and $_p$YfiN I$_{ps}$ were incubated with [α-32P] GTP for 5-

813 minute intervals from 0-15 minutes, and analyzed using TLC (see Methods); only the 10 min data are
814 shown (see text). Each replicate was normalized to initial GTP levels set at 100%. *(E)* As in *D,* but with
815 lysates of cells expressing $_{p}$YfiN and $_{p}$DgcA. *(F)* Absolute quantification of GTP levels in cells expressing
816 indicated plasmids (see Methods). Concentration of GTP for each biological replicate was normalized
817 to wet weight of *E. coli* cells.

818

819

820

821

822

823

824

825

826

827

828

829

830

831

832

833

834

835

836

837

838

839

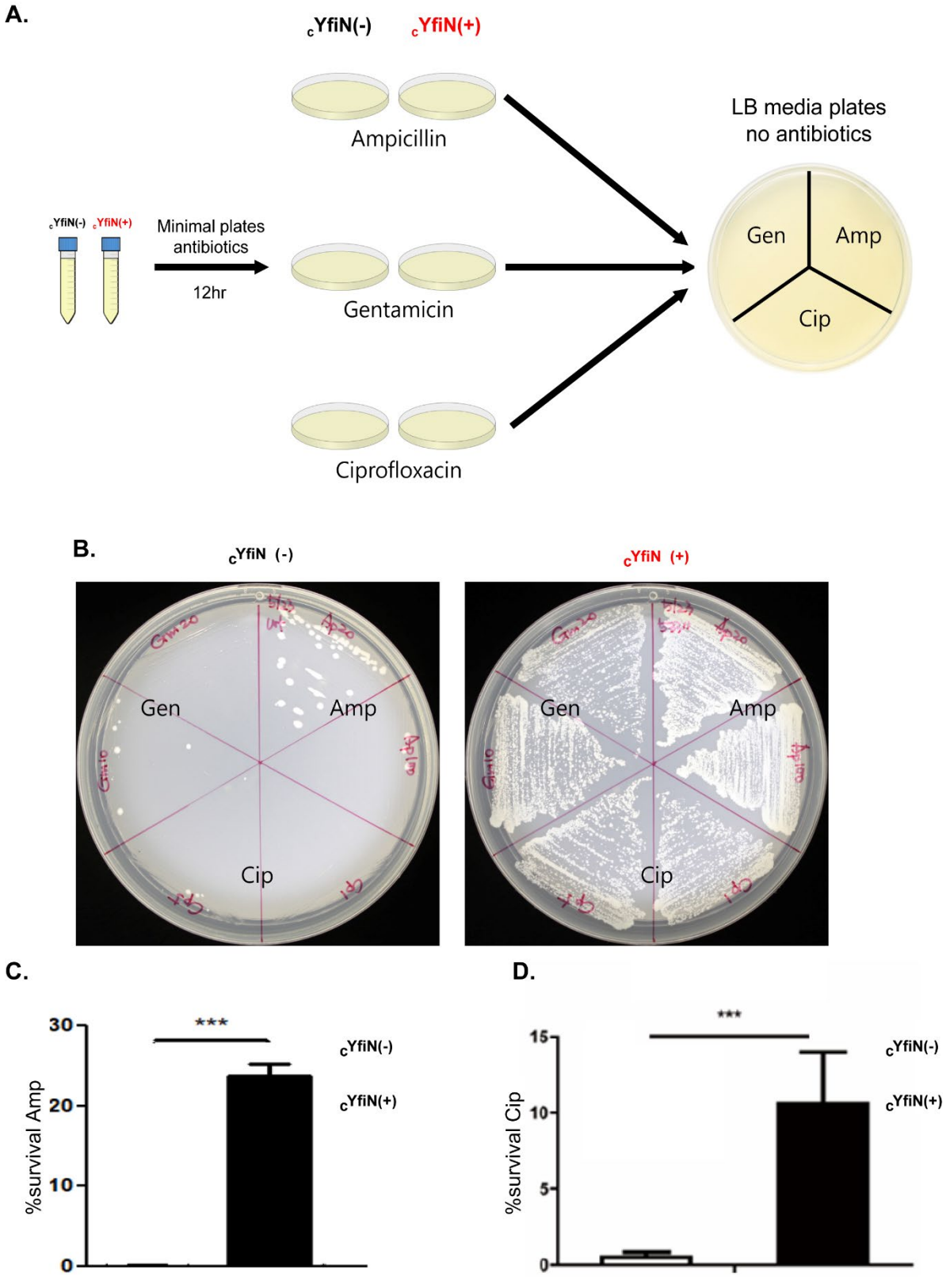

Figure 5. YfiN increases tolerance to different classes of antibiotics. *(A)* Experimental design. (cYfiN$_{GFP}$)-expressing cells grown with or without inducer (+/-) in liquid M9M media were plated on M9M plates supplemented with two different antibiotic concentrations: Ampicillin (Amp; 20 & 100ug/ml), Gentamicin (Gen; 4 & 20ug/ml), Ciprofloxacin (Cip; 2 & 10ug/ml). After overnight incubation, inoculating

845 loops were used to transfer cells to fresh LB plates without antibiotics. The results are shown in *(B)*.
846 Note that there are no antibiotics in the plates shown in B; the labels merely indicate the antibiotic they
847 were treated with on the M9 plates prior to inoculation on the LB plates. *(C-D)* In a separate set of
848 experiments, cells grown with or without YfiN (cYfiN$_{GFP}$) in M9M liquid media for 3 hours were exposed
849 to (*C*) Amp (100ug/ml) or (*D*) Cip (10ug/ml) for 4 hours, before plating on LB. % survival under the three
850 conditions was determined by measuring CFU counts before and after exposure to antibiotics.

851

852

853

854

855

856

857

858

859

860

861

862

863

864

865

866

867

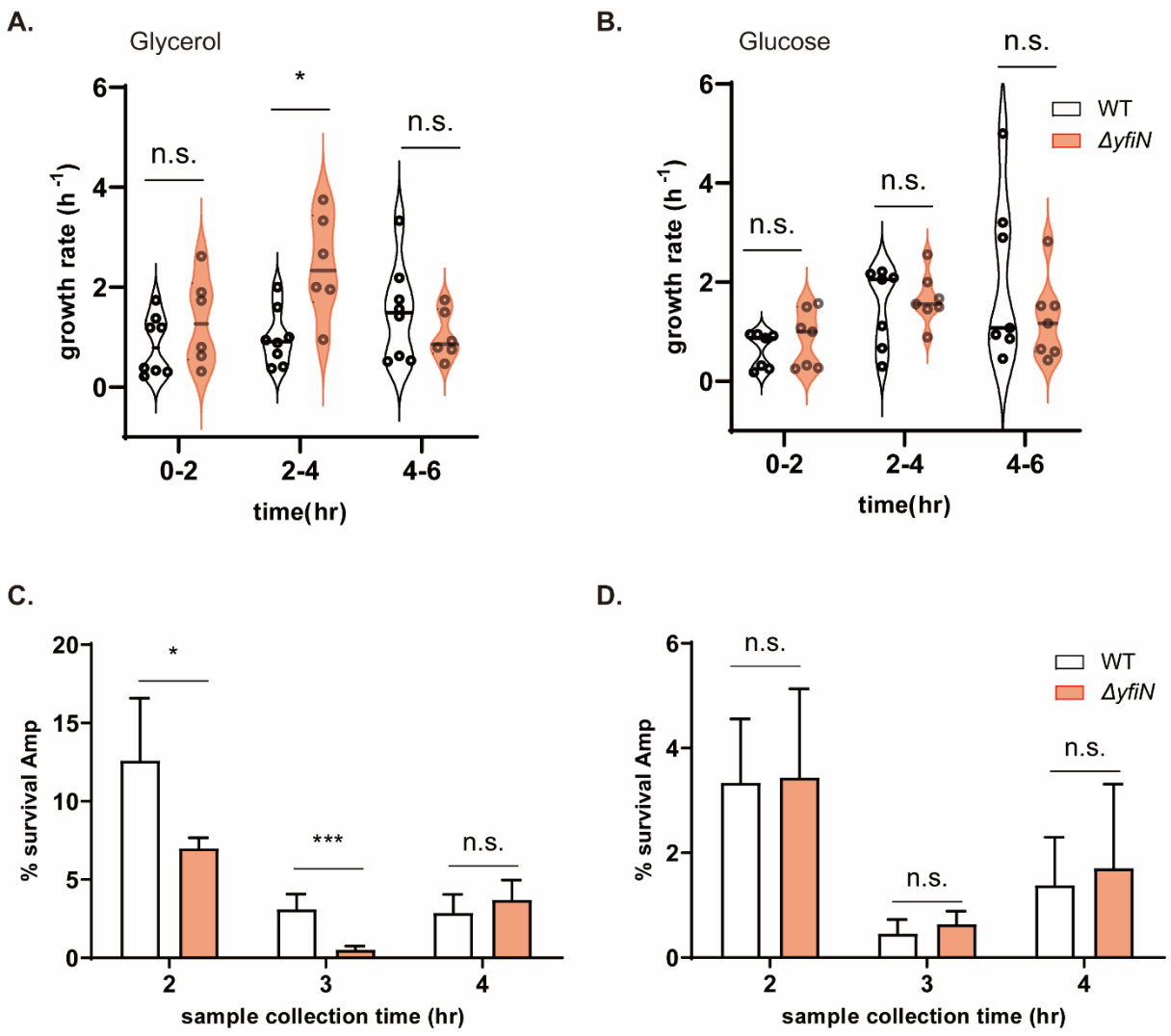

Figure 6. Native YfiN increases the duration of the lag phase of growth. (*A-B*) WT versus *ΔyfiN* strains were grown overnight in LB and inoculated in either M9 glycerol or glucose. Growth rates in the M9 media were calculated using CFUs measured at each time interval shown (see Growth Rate Calculation under Methods). Each black circle is a biological replicate (n=8 glycerol, n=7 glucose). (*C-D*) WT and *ΔyfiN* strains were grown in M9 glycerol or glucose for 0-4 hours and aliquots removed at 2, 3, and 4 hours (within the time windows monitored in A), and treated with Ampicillin (100µg/ml) for 4 hours. At each time, % survival was calculated by comparing CFU counts before and after antibiotic treatment.

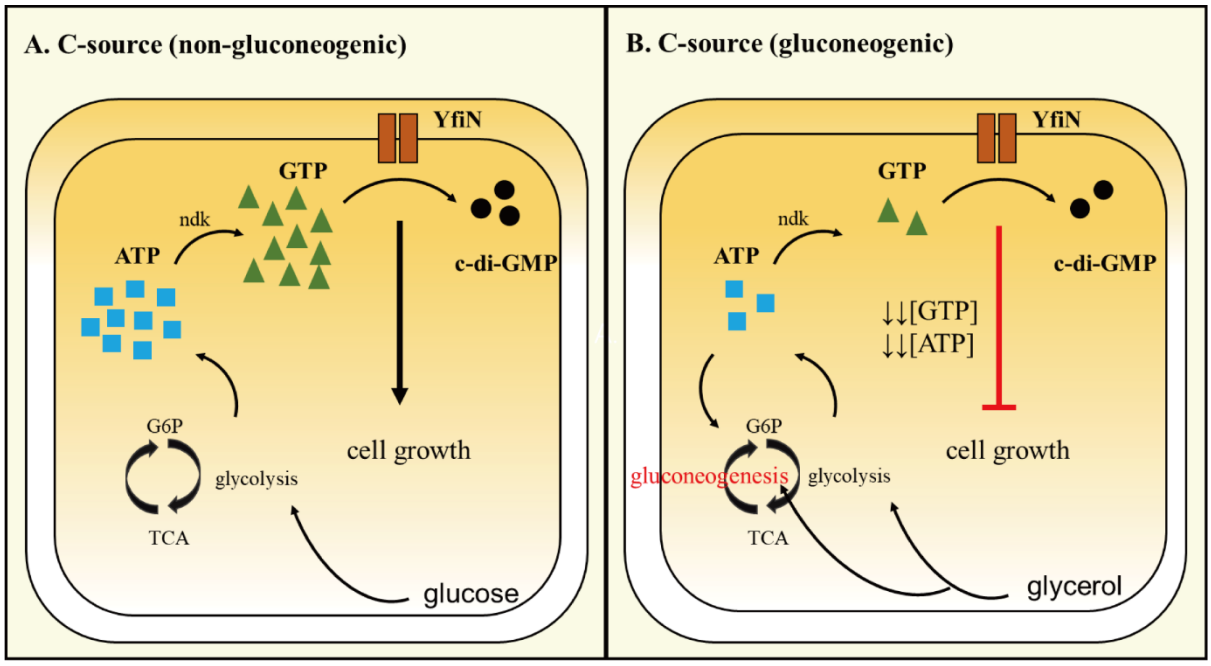

Figure 7. Model for mechanism of YfiN-mediated growth arrest on gluconeogenic carbon (C) sources. (*A*) On glycolytic substrates or rich media, GTP consumption by YfiN does not deplete NTP pools because they are abundant. (*B*) On non-gluconeogenic carbon sources NTP pools are low to begin with, and easily depleted by YfiN activity.

903 **Supplementary Figures and Tables**

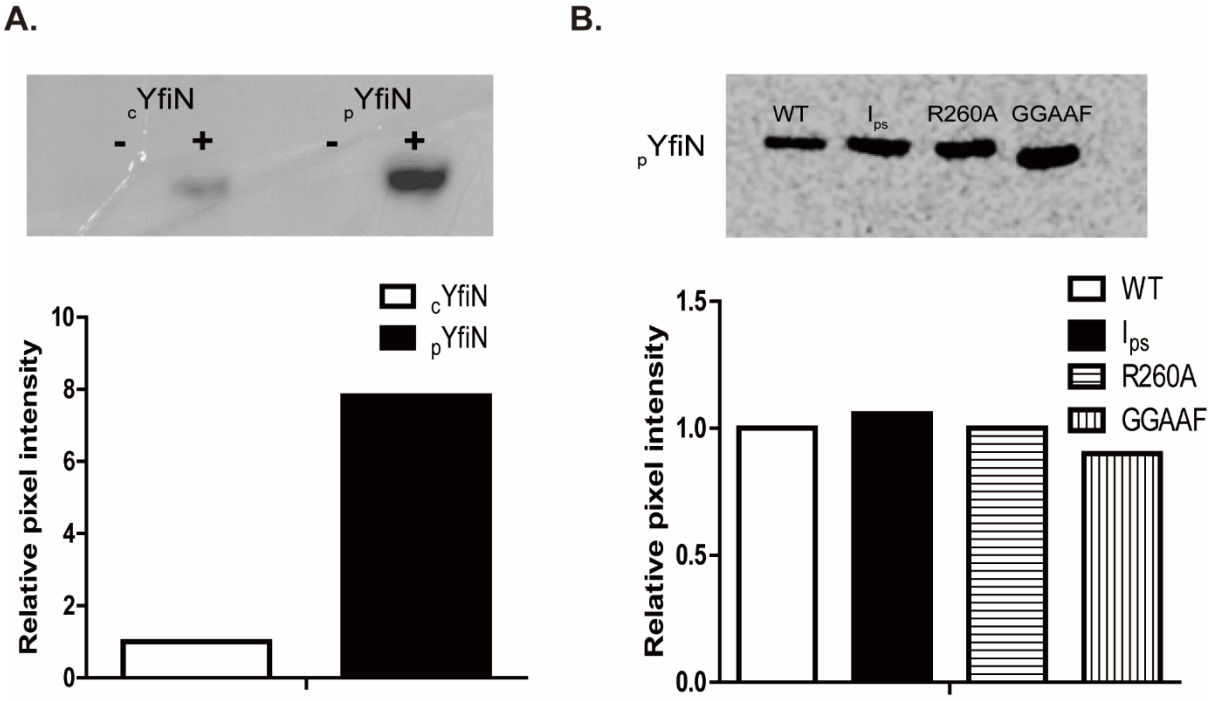

904

905 **Figure S1**. **Comparison of protein expression in different YfiN constructs.** (*A*) A western blot image
906 of cells expressing cYfiN- or pYfiN-GFP, propagated in M9M with 0.02% arabinose. The image was
907 taken using ChemiDoc and pixel intensities (plotted below) were measured with ImageJ software (see
908 Methods). Intensities were normalized to cYfiN. (*B*) As in *A*, except using Flag-tagged pYfiN(WT),
909 pYfiN(I_{ps}), pYfiN(R260A), and pYfiN(GGAAF), with intensities normalized to pYfiN(WT). The intensities
910 are an average from two replicates.

911

912

913

914

915

916

917

918

919

920

921

922

923

924

925

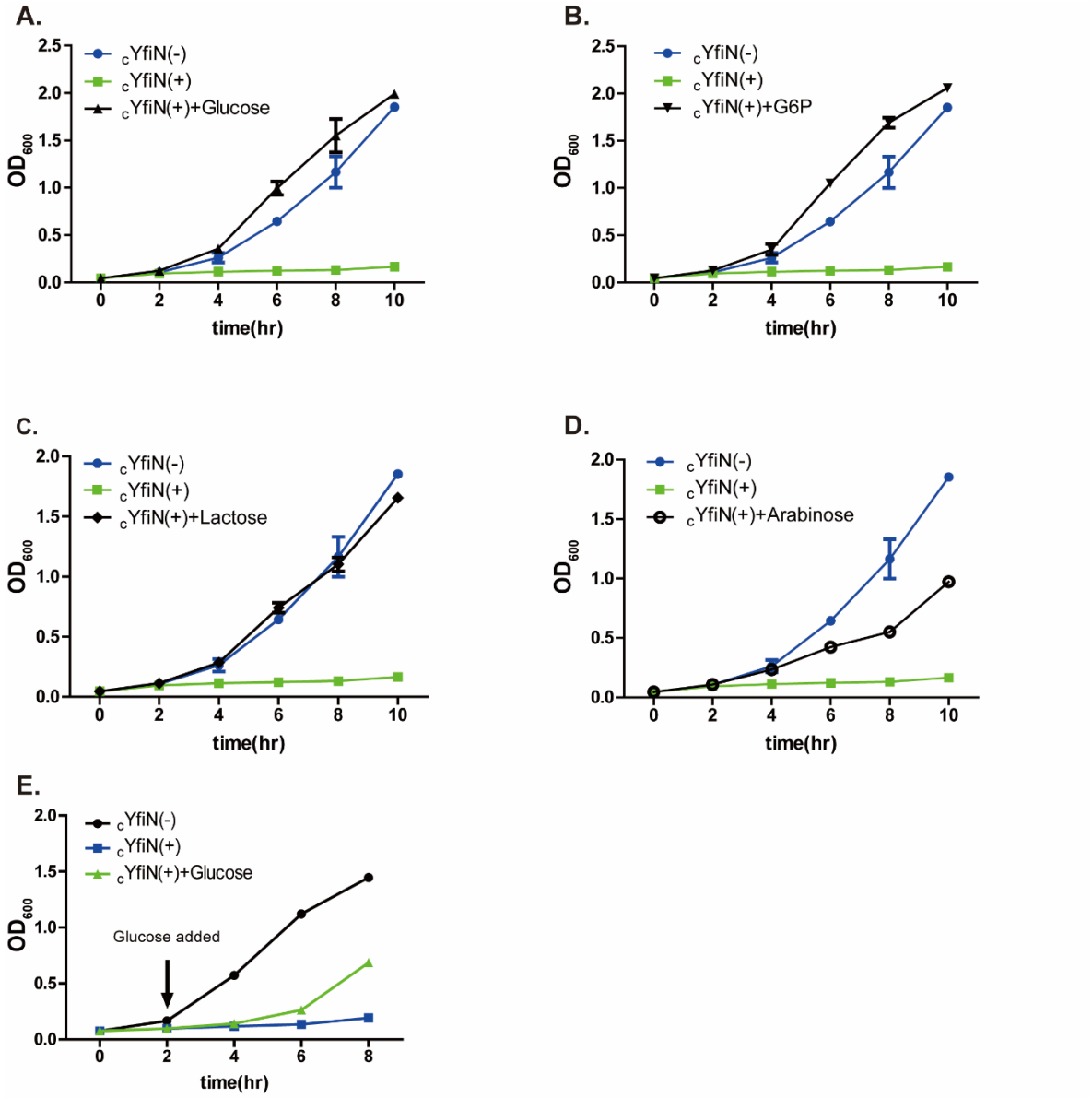

Figure S2. Glycolytic sugars rescue growth-arrest caused by gluconeogenic sugars. *(A-D)* Cells expressing $cYfiN_{GFP}$ were propagated in glycerol alone or in combination with glycolytic substrates (glycerol is present in all experiments, hence not indicated) *(E)* The cYfiN strain was propagated in M9M, and glucose was added at 2 hours post induction. All substrates were at 0.2% w/v. Induction conditions as in Fig. 1.

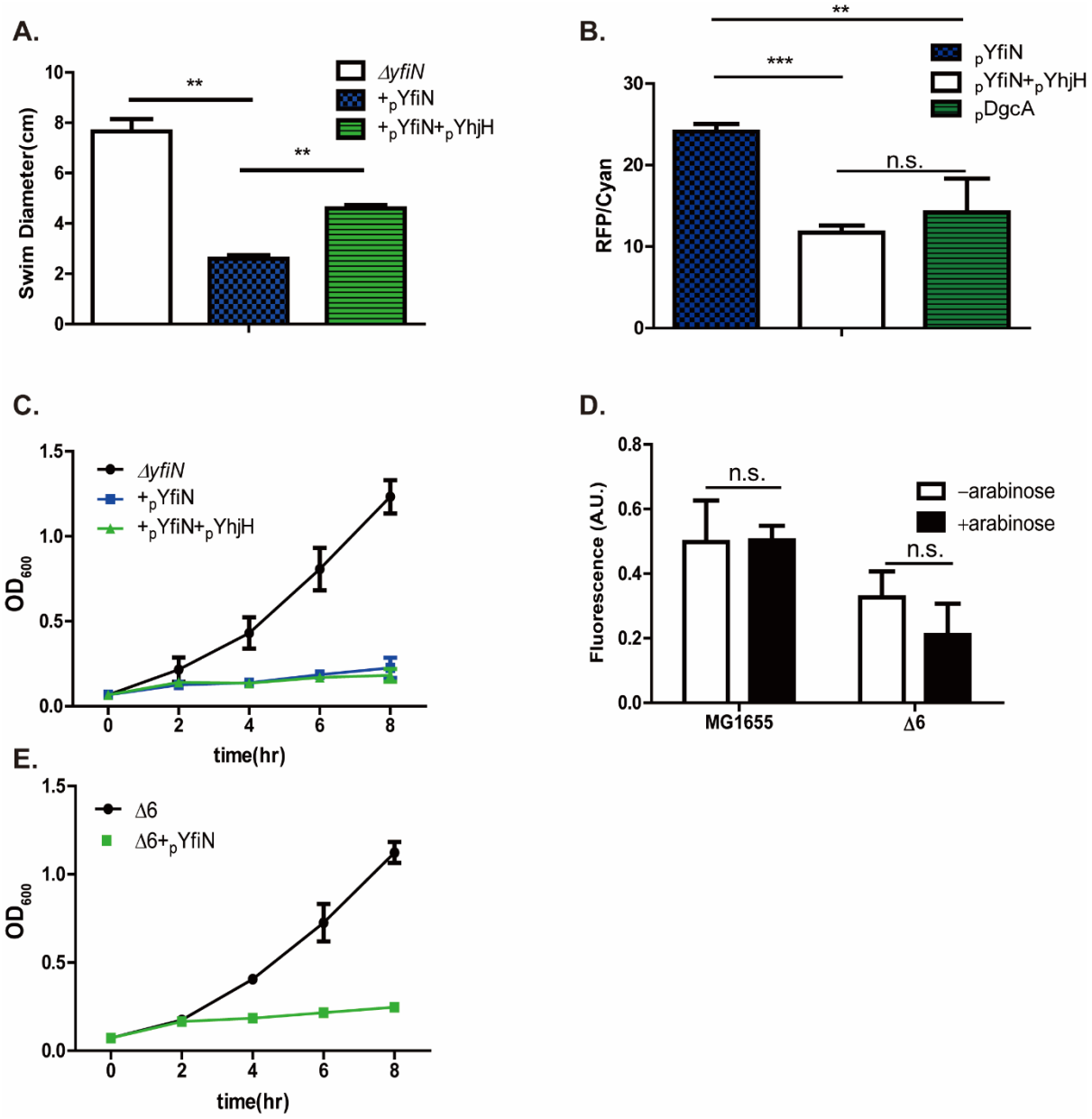

936

937 **Figure S3. The growth-arrest phenotype of YfiN is unrelated to its motility or biofilm output.** (*A*)
938 pYfiN or pYfiN+pYhjH were introduced into the Δ*yfiN* strain and expression induced with arabinose, or
939 arabinose+IPTG, respectively. Motility was measured by estimating the diameter of the swim colony in
940 soft agar plates. *(B)* c-di-GMP levels for $_p$YfiN, $_p$YfiN + $_p$YhjH, and $_p$DgcA were measured using a
941 riboswitch-based fluorescent biosensor, where CFP is expressed constitutively and RFP is the readout
942 for c-di-GMP; the RFP/CFP ratio estimates c-di-GMP/cell (see Methods). The data were obtained from
943 four biological replicates of each sample. (*C*) Strains in *A* were monitored for growth in M9M in the
944 presence of their respective inducers. *D*) The parent MG1655 strain was deleted for six genes that
945 control all the biofilm pathways in *E. coli* (Δ6 = *bcsA, csgD, pgaC, fimA, wcaD, yjbE*). pYfiN was
946 introduced in both strains and the amount of biofilm formed was estimated by Crystal violet staining,
947 with or without arabinose in 96 well plates. A.U., arbitrary fluorescence units. (*E*) Strains in *D* were
948 monitored for growth in M9M in the presence of arabinose.

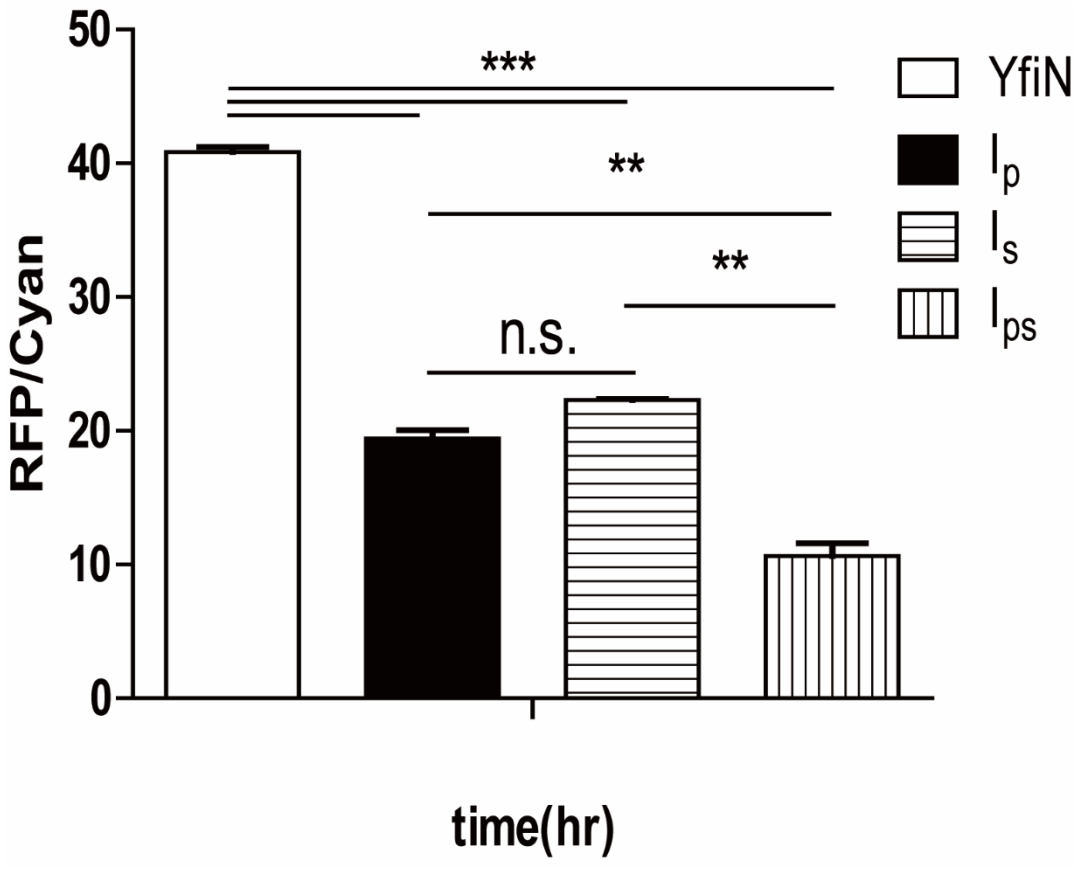

Figure S4. **Comparison of c-di-GMP levels in cells expressing pYfiN and its I site mutants I_p, I_s, I_{ps}.** The data were obtained by using a riboswitch-based fluorescent biosensor as described in Fig. S3B.

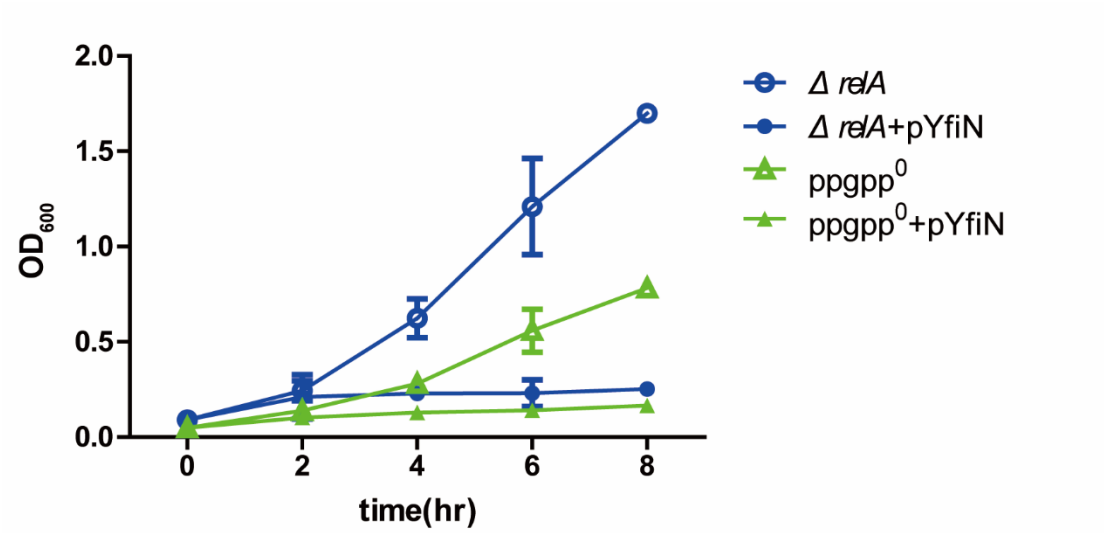

Figure S5. The (p)ppGpp pathway does not contribute to YfiN-mediated growth arrest. Time course growth of *ΔrelA* or *ΔrelAΔspoT*(ppGpp^0) strains transformed with pYfiN and propagated in M9M with 0.02% arabinose.

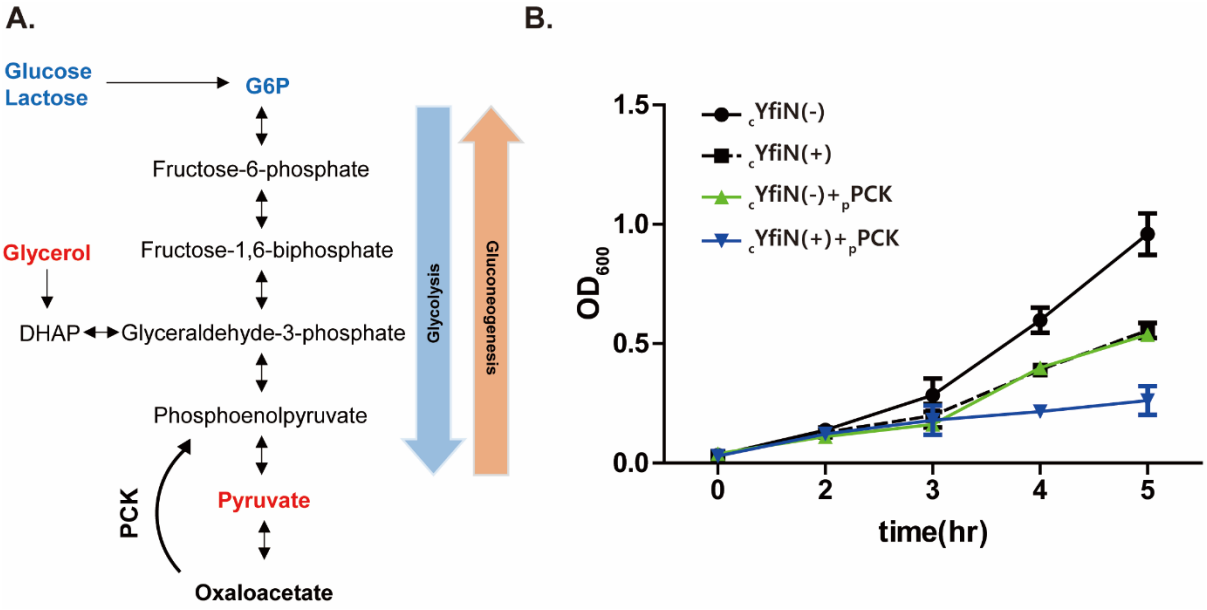

Figure S6 Co-expression of PCK with cYfiN$_{GFP}$ increases severity of growth arrest. *(A)* Gluconeogenesis pathway indicating the step at which PCK acts. *(B)* Growth curve in M9 mannitol of the $_{c}$YfiN$_{GFP}$ (induced with arabinose: -/+) and strain transformed with pPCK (induced with IPTG).

1004

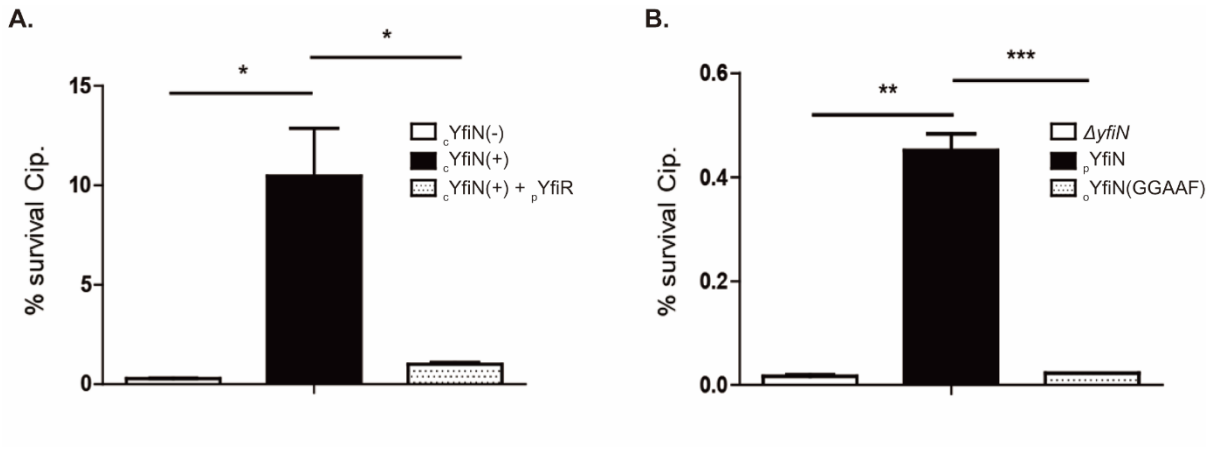

1005

1006 **Figure S7 The DGC activity of YfiN is essential for antibiotic tolerance.** (*A*) The cYfiN$_{GFP}$ strain was
1007 transformed with pYfiR (periplasmic inhibitor of YfiN) and induced with IPTG or arabinose, respectively.
1008 Cells were propagated in M9M for 4 hours before addition of Cip (20µg/ml) to the media. After incubation
1009 for 4 hours, % survival was determined by measuring CFU counts before and after antibiotic exposure.
1010 (*B*) As in *A* except with pYfiN and its active site mutants. The lower cell survival in B vs A is likely due
1011 to higher GTP depletion in pYfiN compared to cYfiN, leading to higher toxicity and cell death [58].

1012

1013

1014

1015

1016

1017

1018

1019

1020

1021

1022

1023

1024

1025

1026

1027

1028

1029

1030

1031

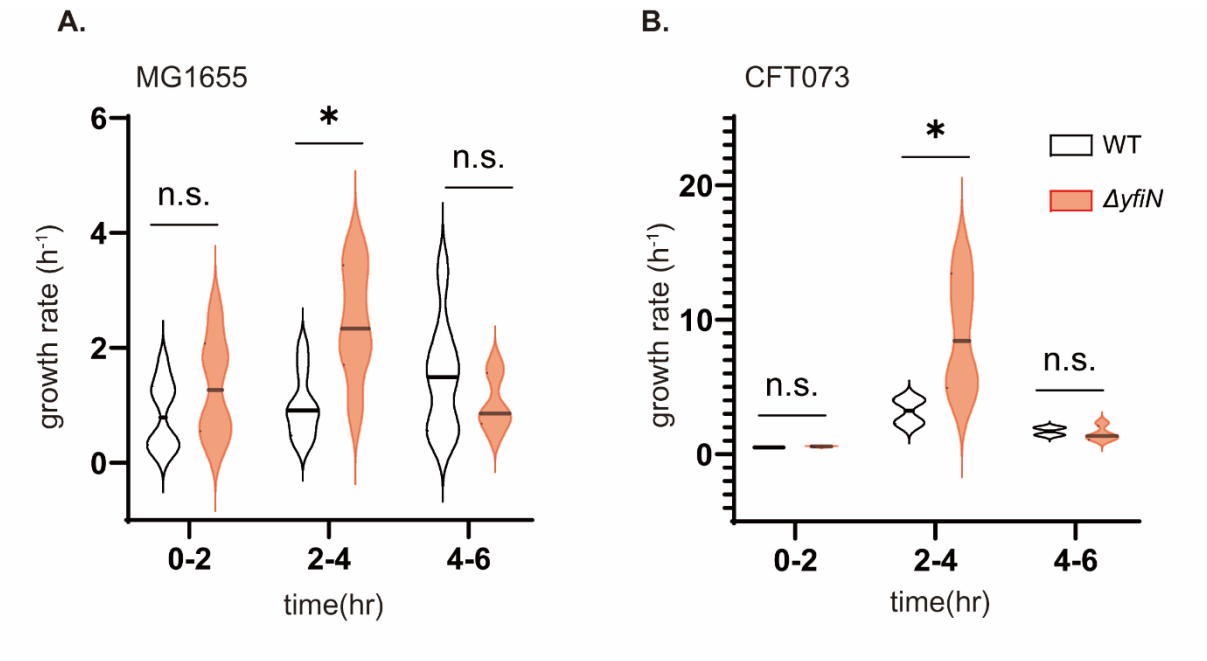

Figure S8. Growth rate comparisons of two *E. coli* WT strains and their *ΔyfiN* derivatives in M9 glycerol. *(A)* Data for the WT lab strain MG1655 are taken from Fig. 6A (n=8). *(B)* Similar experiments, but with the uropathogenic strain CFT073 (n=4).

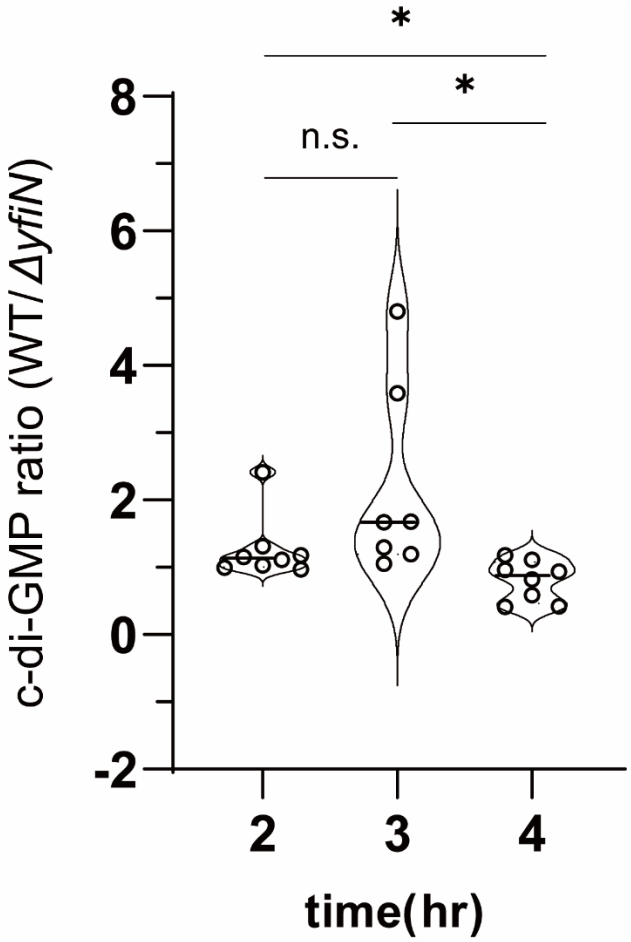

Figure S9. c-di-GMP levels in WT vs. ΔYfiN measured by the riboswitch-based biosensor. The strains were propagated in M9M and fluorescence measured as in Fig. S3B. Samples collected at indicated time points were diluted to OD_{600} of 0.5, prior to measurement. Each dot represents one biological replicate (n=8 for 2 & 4 hours , and 7 for 3 hours).

		I_s					I_p									Active site				
PleD(C.crescentus)	K	R	A	T	···	R	A	I	D	L	P	C	R	Y	G	G	E	E	F
YfiN(Y.frederiksenii)	K	D	C	-	···	R	E	S	D	L	V	A	R	L	G	G	D	E	F
YfiN(Y.intermedia)	S	D	C	-	···	R	E	T	D	L	V	A	R	L	G	G	D	E	F
YfiN(P.fluorescens)	R	S	A	A	···	R	E	D	D	L	V	A	R	L	G	G	D	E	F
YfiN(P.aeruginosa)	R	D	A	N	···	R	E	S	D	L	V	A	R	L	G	G	D	E	F
Consensus		R				R	X	X	D						G	G	D	E	F

Figure S10 YfiN homologs that have I_p but not I_s sites. The I_p site (RXXD), the predicted I_s site (R), and the DGC active site (GGDEF) are boxed in a sequence alignment of YfiN from *Yersinia* (Y) and *Pseudomonas* (P) species, and compared to PleD from *C. crescentus*, which has a functional set of both I sites (see Fig. 3B).

1080 **Table S1**

Strains	Genotype or Description	Reference
MG1655	K12 wild-type (WT) strain: F^- , λ^- , rph-1	Laboratory Collection
HK359	MG1655 Δ*yfiN*	[24]
HK461	HK359 + pBAD30_YfiN$_{GFP}$	[24]
JH101	HK359 + pBAD30_YfiN	This study
HK532	MG1655 yfiR::kan(←) yfiN::pBAD-*yfiN-gfp*	[24]
HK533	MG1655 yfiR::kan(←) yfiN::pTrc-*yfiN-gfp*	This study
HK800	HK359 + pBAD33_YfiN$_{GFP}$	
JH102	MG1655 + pBAD33_DgcA	This study
JH100	HK359 + pBAD30_YfiN	This study
JH103	HK359 + pBAD30_YfiN(GGAAF)	This study
JH104	HK359 + pBAD30_YfiN(I_p)	This study
JH105	HK359 + pBAD30_YfiN(I_s)	This study
JH106	HK359 + pBAD30_YfiN(I_{ps})	This study
JH107	MG1655 + pBAD33_DgcA(GESD)	This study
JH108	HK359 + pBAD33_YfiN(R260A)$_{GFP}$	This study
JH109	HK532 + ASKA_PCK	This study
JH202	MG1655 + pBAD33_DgcC	This study
JH203	MG1655 + pBAD33_DgcE	This study
JH204	MG1655 + pBAD33_DgcF	This study
JH201	MG1655 + pBAD33_DgcJ	This study
JP1932	AW405 Δ*bcsA csgD pgaC fimA wcaD yjbE*	[32]
JH110	HK359 + pBAD33_YfiN + pTrc99a_YhjH	This study
JH111	HK532 + pTrc99a_YfiR	This study
JH250	HK359 + pBAD30_YfiN-Flag (c-term.)	This study
JH251	HK359 + pBAD30_YfiN(I_{ps})-Flag (c-term.)	This study
JH252	HK359 + pBAD30_YfiN(GGAAF)-Flag (c-term.)	This study
JH253	HK359 + pBAD30_YfiN(R260A)-Flag (c-term.)	This study

JH300	HK359 + pBAD30_YfiN-Flag(c-term.)	This study
JH301	HK359 + pBAD30_YfiN + pFY4535	This study
JH302	HK359 + pBAD30_YfiN(I_p) + pFY4535	This study
JH303	HK359 + pBAD30_YfiN(I_s) + pFY4535	This study
JH304	HK359 + pBAD30_YfiN(I_{ps}) + pFY4535	This study
JH305	MG1655 + pFY4535	This study
JH306	HK359 + pFY4535	This study
JH307	JH110 + pFY4535	This study
JH308	HK359 + pBAD33_YfiN + pTrc99a_Empty + pFY4535	This study
JH309	JH102 + pFY4535	This study
CFT073	Uropathogenic strain of *E. coli*	R. Welch, U. Wisconsin-Madison
HK701	CFT073Δ*yfiN*	Hyo Kyung Kim
Plasmids	Expressed Proteins	Reference
pKD4	Kanamycin resistance gene template	[66]
pKD46	λ Red Recombinase	[66]
pCP20	FLP recombinase	[66, 69]
pTrc99a	Cloning vector, P_{Trc}; Amp^R	[69, 70]
pBAD30	Cloning vector; P_{BAD}; Amp^R	[70]
pBAD33	Cloning vector; P_{BAD}; Cm^R	[24, 70]
pBAD30_$YfiN_{GFP}$	pBAD::YfiN-GFP(C-terminal)	[24]
pBAD30_YfiN	pBAD::YfiN	This study
pBAD33_YfiN	pBAD:;YfiN	This study
pBAD30_YfiN(GGAAF)	pBAD:: YfiN (D329A E330A)	This study
pBAD30_YfiN(Ip)	pBAD::YfiN (G317R H320D)	This study
pBAD30_YfiN(Is)	pBAD::YfiN (N280R)	This study
pBAD30_YfiN(Ips)	pBAD::YfiN (N280R G317R H320D)	This study

pBAD33_DgcA	pBAD::DgcA	This study
pBAD33_DgcA(GESD)	pBAD::DgcA (R80G)	This study
pBAD30_YfiN(R260A)$_{GFP}$	pBAD::YfiN (R260A)-GFP	Hyo Kyung Kim
pBAD30_YfiN-Flag (c-term.)	pBAD::YfiN-Flag	This study
pBAD30_YfiN(I_{ps})-Flag (c-term.)	pBAD:: YfiN(I_{ps})-Flag	This study
pBAD30_YfiN(GGAAF)-Flag (c-term.)	pBAD:: YfiN(GGAAF)-Flag	This study
pBAD30_YfiN(R260A)-Flag (c-term.)	pBAD:: YfiN(R260A)-Flag	This study
pFY4535_pmmb-bc3-5-phok-sok	pMMBGent::c-di-GMP sensor	[34]
pBAD33_DgcC	pBAD::DgcC	This study
pBAD33_DgcE	pBAD::DgcE	This study
pBAD33_DgcF	pBAD::DgcF	This study
pBAD33_DgcJ	pBAD::DgcJ	This study
pTrc99a_Empty	pTrc99a::Empty	This study
pTrc99a_YhjH	pTrc::YhjH	This study
pTrc99a_YfiR	pTrc::YfiR	This study

1081